FACULTY OF PSYCHOLOGY AND EDUCATIONAL SCIENCES

Simulating depression-like abnormal brain activity and stimulation treatment with The Virtual Brain

Word count: 12108

Celien Iliaens
Student number: 01508943

Supervisor(s): Prof. Dr. Daniele Marinazzo

A dissertation submitted to Ghent University to obtain the degree of Master of Science in Psychology, option Theoretical and Experimental Psychology

Academic year: 2020-2021

GHENT UNIVERSITY

Acknowledgements

Getting to know the world of computational modelling and applying it to write this thesis has been a challenging journey that would not have been as successful without some support. First, I would like to thank Prof. Dr. Daniele Marinazzo very much for his guidance and his constant availability when needed during this project. Working with such an expert in the field not only helped me to carry out the current project, it also allowed me to learn a lot about modelling and data analyses in a broader context. Next, I would like to thank my family for the mental support during the hard times. Finally, for that same reason I want to express my thanks to my friends. It is so much easier to carry on during difficult times when you know you are not alone.

Abstract

Major depressive disorder is a severe mental health issue affecting many people. Previous research found evidence for changes in functional and structural connectivity as well as changes in neurotransmitters in the brain of depressed patients. However, the literature on these changes is often contradictory. In the current study we make use of a modelling approach to study the changes in depressed brains and the effects of non-invasive brain simulation interventions using The Virtual Brain (TVB). TVB is a neuroinformatics platform that builds a personal virtual brain for each individual subject based on individual tractographic data and general neural mass models. Based on this individual virtual brain, output in the form of functional imaging data can be produced. Due to the lack of real patient data, we simulated 100 healthy brains based on the default connectivity matrix included in TVB using the Wilson-Cowan model. Next, we simulated 100 depressed brains by adjusting local inhibition in crucial regions. Finally, we simulated low-frequency rTMS (LF-rTMS) treatment (n=100) and high-frequency rTMS (HF-rTMS) treatment (n=100) applied to the baseline depressed brains. We then compared alpha power, frontal alpha asymmetry and coherence between the four groups of brain types in order to investigate 1) whether the differences between the depressed and healthy virtual brain are in line with literature, 2) whether the rTMS protocols could cause treatment-like effects and 3) if so, whether one treatment protocol would be superior compared to the other. Results were ambiguous and not completely in line with expectations based on literature. Specifically, we could not always find the predicted differences between healthy and depressed brains and treatment-like effects caused by HF-rTMS and/or LF-rTMS were scarce. Moreover, we did not find evidence pointing towards one treatment as being superior to the other. We argue that our model for the depressed brain might be too simplistic and encourage the use of real patient data in TVB for future research. Finally, we highlight some issues of inconsistencies across studies which might underly the diverse conclusions in literature.

Keywords: The Virtual Brain, Wilson-Cowan model, depression, rTMS

Table Of Content

Contents

Acknowledgements 2
Abstract 3
Table Of Content 4
The brain as a network 5
The virtual brain 6
Dynamical systems theory 8
Wilson-Cowan model 10
The Depressed Brain 11
Non-invasive brain stimulation 16
Current study 18
Method 19
Materials 19
Simulating virtual brains 19
Data analyses 22
Results 24
Frontal alpha power 24
Alpha peak 26
Coherence 29
Discussion 34
Frontal alpha power 34
Alpha peak 37
Coherence 38
General discussion 39
Conclusion 40
References 41
Appendix A 60
Appendix B 61
Appendix C 62
Appendix D 63
Dutch summary 64

The brain as a network

With its ~10^{11} neurons and ~10^{15} connections (Ritter et al., 2013) our brain is our most complex organ of which many mechanisms are not yet understood. With the emergence of new non-invasive neuro-imaging techniques and their resulting large datasets, a great way of studying the brain is by making use of complex network analysis.

Complex network analysis is derived from graph theory, which was first used in mathematics and sociology but later found application in a wide range of domains, such as neurology (Mulders et al., 2016). Graph theory describes networks as consisting of nodes and edges (links). When applied to neuroscience, nodes can represent single neurons or even entire brain-regions whereas the edges represent the connectivity between these regions. Such connections could be structural (white matter fibers, synapses) or functional (correlation between time series) (Dwyer et al., 2016). In contrast to classical graph theory, complex network analysis describes real-life networks that are large and complex (Rubinov & Sporns, 2010).

When applied to brain data, an important distinction between structural and functional networks is made. Structural networks reflect anatomical connections in the brain (Sporns, 2014; Sporns & Betzel, 2016) which can be retrieved using DTI (i.e. diffusion tensor imaging). These white-matter connections are fixed on a short time scale, but can change over longer periods of time due to neuronal growth or learning (Stam et al., 2016). On the other hand, functional networks are based on correlations among time series of neural activity (Friston 2011; Park & Friston, 2013; Sporns, 2014; Sporns & Betzel, 2016) and are most commonly retrieved using resting state fMRI (rsfMRI). Individual differences in both structural networks (Klein et al., 2016; Li et al., 2009; Matejko et al., 2013; Willmes et al., 2016) and functional networks (Ferguson et al., 2017; Hearne et al., 2016; Song et al., 2008; Van Den Heuvel et al., 2009) have been associated with a variety of cognitive functions. Moreover, alterations in these networks have been found in a range of neurological and affective disorders (Baggio et al., 2014; Jacobs et al., 2012; Lo et al., 2010; Filippi & Agosta, 2011; Rotarska-Jagiela et al., 2010; Wu et al., 2017). For example, both alterations in structural (Ajilore et al., 2014; Lim et al., 2013; Long et al., 2015) and functional (Greicius et al., 2007; Kaiser et al., 2016; Peng et al., 2012; Sheline et al., 2010; Wu et al., 2017) connectivity have been reported in people suffering from depressive disorders.

To really understand the functional networks (Honey et al., 2010; Marrelec et al., 2016) and ultimately to understand cognition and behaviour (Sporns, 2011), the structural network is of great importance. For instance, it has been demonstrated that the structural network places constraints on the possible functional interactions in a network (Bullmore & Sporns, 2009; Park & Friston, 2013; Sporns, 2011). However, the exact link between structural and functional brain connectivity is not yet completely understood. The Virtual Brain (TVB; Jirsa et al., 2010), a neuroinformatics platform, can be of great help in studying both structural and functional connectivity as well as the relation between them.

The virtual brain

Given the gap between the microscale (describing individual neurons and their action potentials) and the macroscopic data (obtained through neuroimaging), a neural model aiming to describe the activity of single neurons has far too many degrees of freedom to be capable of finding a good fit with macroscopic data. However, a concept from physics pointed out that macroscopic physical systems follow laws that are independent of the specific underlying microscopic elements on which the systems were build (Haken, 1975; Ritter et al., 2013). This gave rise to the introduction of a mesoscale in neuroscience, describing the activity of populations of neurons and thus forming a bridge between the micro- and macroscale.

Neural mass models, which model the activity of groups of neurons, can thus be situated at this mesoscale. These models assume that for the analysis of complex neural dynamics at the mesoscale it is not necessary to look at the specific underlying structural and functional elements at the microscale (Ritter et al., 2013). Following this assumption, these models postulate that behaviour and cognition only partly depend on the specific underlying individual neuronal activity (Breakspear & Jirsa, 2007; Ritter et al., 2013).

The Virtual Brain uses such neural mass models to describe the dynamics of each node or region of interest (i.e. ROI) in a biologically plausible way (Ritter et al., 2013). Furthermore, TVB uses individual tractographic data, retrieved with diffusion tensor imaging (i.e. DTI). Based on the tractographic data, a connectivity matrix is created containing the connection strengths and time delays between all network nodes

(Leon et al., 2013b). By combining neural mass models with the personal connectivity matrix, TVB can create an individual virtual brain for each subject (Solodkin et al., 2018). Furthermore, it can be used to simulate realistic Local Field Potentials (LFP) and brain imaging data such as electroencephalography (EEG) data, functional magnetic resonance imaging (fMRI) data and magnetoencephalography (MEG) data (figure 1).

Because TVB is based on personal tractographic data, it is possible to create personal virtual brains for each subject. It is thereby feasible to study how certain model parameters correlate with clinical phenotypes (Solodkin et al., 2018). For example, Zimmermann and colleagues (2018) found that their modelled local (excitation, inhibition) and global (long-range coupling, conduction velocity) brain dynamics correlated well with individual cognition in Alzheimer's disease.

Another great advantage of TVB is that it allows manipulation to whole-brain dynamics, for example through stimulation. There are two kinds of stimulations in TVB: surface-based and region-based stimulation. In surface-based stimulation, each vertex on the surface is described as a node whereas in region-based stimulation each node represents a specific brain region (Leon et al., 2013a). The user can apply such stimulations and subsequently assess the consequences of the stimulation on the personalised virtual brain.

Finally, TVB is open-source and, being based on Python, easy to use.

Figure 1

Overview of the functioning of TVB

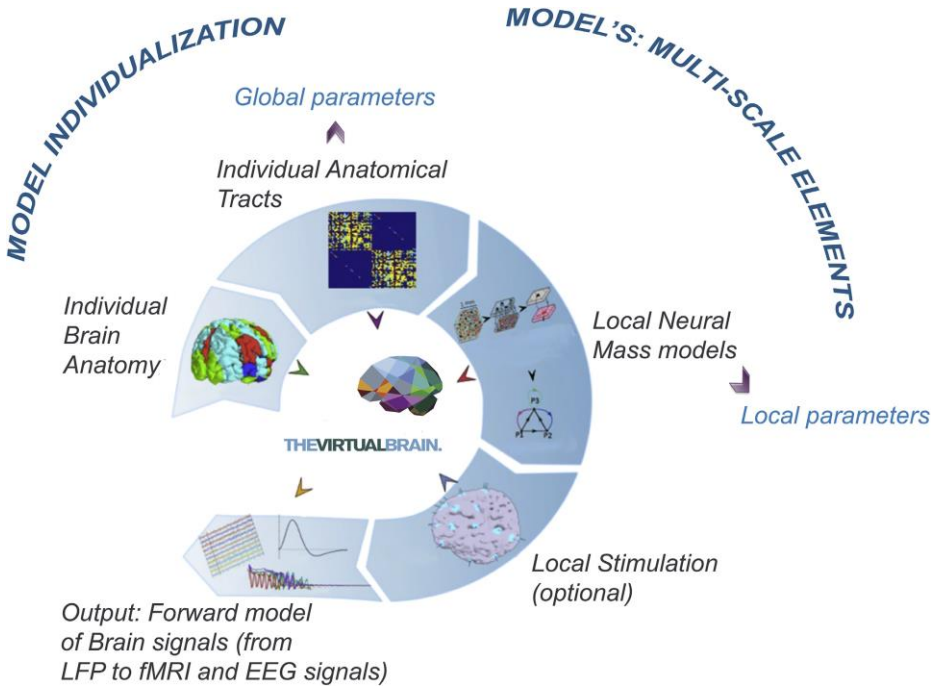

Note. Retrieved from Solodkin et al. (2018). Individual Brain anatomy is acquired and used to create an individual connectivity matrix**.** Afterwards, local neural mass models are chosen and combined with the individual connectivity matrix to create an individual Virtual Brain. If wanted, there is an option to add stimulation to specific brain nodes. Using a forward model, the simulated output can be obtained in the form of LFP, EEG, MEG or BOLD signals.

Dynamical systems theory

Such neural mass models as used in TVB rely on the dynamical systems theory. Dynamical systems theory is a mathematical theory that describes complex dynamical systems, usually by means of differential equations (in which case we speak of continuous dynamical systems)(e.g., Landa, 2013, Strogatz, 2018). A dynamical system, defined by *m* state variables, has a state that can be described by a point in an *m*-dimensional space: the state space or phase plane. The evolution of the dynamical system is determined through a fixed rule, namely a set of differential equations where each equation represents one of the system variables. This set of equations then

describes the future state the system will evolve to depending on the current state. The evolution of the system over time is called the trajectory.

The system, which applied to neuroscience could represent a neuron or a group of neurons, is excitable because it is near a transition (i.e., bifurcation): from resting to sustained spiking activity (Izhikevich, 2007). A system at rest is defined as a system where no changes in state variables occur (Izhikevich, 2007). Such a system is located in an equilibrium. When the system remains at rest despite of small disturbances, we speak of a stable equilibrium (figure 2). However, when such small disturbances are enough to cause changes in the system, the equilibrium was unstable (figure 2) (Izhikevich, 2007).

Trajectories are attracted by such stable equilibria (i.e., attractors) and move away from so-called repellers. An attractor can either be a single fixed point or a limit cycle. In the case of a fixed point attractor, trajectories are attracted to one specific point in which the system is stable. Such an attractor gives rise to dampened oscillations. Specifically, while the system is moving toward the attractor oscillations occur whereas these oscillations stop after the system arrived in the fixed point attractor. On the other hand the trajectory can also be attracted to a limit cycle. In this case, the trajectory forms a closed loop instead of moving towards a fixed point (Izhikevich, 2007). Since the trajectory keeps moving in the loop and doesn't 'stop' in a fixed point, the resulting oscillations are self-sustained.

When modelling neural models it is important to obtain realistic oscillations. Since there are always oscillations going on in the brain it is thus important to adjust the model parameters in such a way that they result in self-sustained oscillations. Specifically, it is thus important that the model parameters give rise to a limit cycle in the phase plane.

Figure 2

Equilibria in the state space

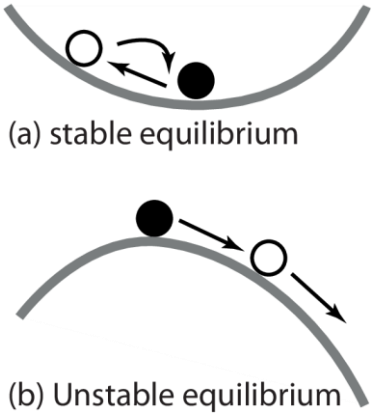

Note. Retrieved from Chadefaux (2010). A) represents a stable equilibrium whereas B) represents an unstable equilibrium.

Wilson-Cowan model

One of the neural mass models implemented in TVB is the Wilson-Cowan model (Wilson & Cowan, 1972; Wilson & Cowan, 1973). This model consists of two neural masses, one of which represents an excitatory population whereas the other one represents an inhibitory population. The activity of these excitatory and inhibitory populations are described by the state variables E and I respectively, which can be formulated as a dynamical unit at a node *k* in a neural mass model with *l* nodes as follows:

$$\dot{E}_k = \frac{1}{\tau_e}\left(-E_k + (k_e - r_e E_k)\mathcal{S}_e\left(\alpha_e\left(c_{ee}E_k - c_{ei}I_k + P_k - \theta_e + \mathbf{\Gamma}(E_k, E_j, u_{kj}) + W_\zeta \cdot E_j + W_\zeta \cdot I_j\right)\right)\right)$$

$$\dot{I}_k = \frac{1}{\tau_i}\left(-I_k + (k_i - r_i I_k)\mathcal{S}_i\left(\alpha_i\left(c_{ie}E_k - c_{ee}I_k + Q_k - \theta_i + \mathbf{\Gamma}(E_k, E_j, u_{kj}) + W_\zeta \cdot E_j + W_\zeta \cdot I_j\right)\right)\right)$$

In these equations, Γ(Ek, Ej, ukj) is the long-range coupling term capturing the input activity of the connected nodes in the network (Sanz Leon et al., 2015). $W_\varsigma \cdot E_j$ and $W_\varsigma \cdot I_j$ represent the activity of inhibitory and excitatory units in the local neighbourhood. E represents the excitatory mass through which the models at each node are linked. r_e and r_i are the refractory periods which are set to zero and k_a, the corresponding activation function, is set to 1 for both populations (Sanz Leon et al., 2015).

Importantly, the Wilson-Cowan model contains parameters which allow us to alter the amount of inhibition and/or excitation in the model. Besides coupling strength variables binding to the same (Cii, Cee) or the other (Cie, Cei) population **(**figure 2, appendix A), we can also alter the variables representing the external inputs to the neural groups. A first one of such variables is P, which represents the external inputs to the excitatory group. Secondly, the Q variable represents the external inputs to the inhibitory group where a reduction in Q thus leads to a reduction in inhibition in the model. The Wilson-Cowan model has already proven to be successful in building biophysically realistic models (Liley et al., 1999, Steyn-Ross et al., 1999, Steyn-Ross et al., 2003, Daffertshofer and van Wijk, 2011; Duchet et al., 2019). For example, Li et al. (2019) were able to observe the typically observed imbalance in excitation/inhibition within the DLPFC by applying the Wilson-Cowan model to rs-fMRI data from depressed patients.

Figure 3

Representation of the Wilson-Cowan model

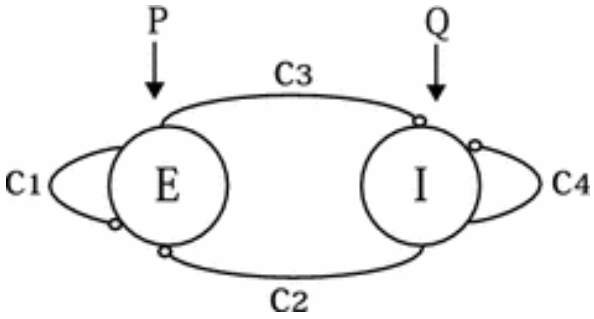

Note. Retrieved from Maruyama et al. (2014). The Wilson-Cowan model consists of an excitatory population (E) and an inhibitory population (I). C1 and C4 are self-coupling variables whereas C2 and C3 are cross-population coupling parameters. The excitatory and inhibitory population receive external input in the form of P and Q respectively.

The Depressed Brain

Major Depressive Disorder (MDD) is a common, severe mental health problem. In addition to a depressive mood, MDD is also characterised by cognitive and somatic symptoms that hinder normal functioning of the patient in his or her daily life (Otte et al., 2016). In the USA, the National Survey on Drug Use and Health, revealed that the life time prevalence of major depressive episode among adults in 2017 was 7.1% (The

National Institute of Mental Health Information Resource Center, 2019). In that same year, depressive disorders had a worldwide prevalence of 3.4% (Ritchie & Roser, 2018) and were the third leading cause of Years Lived with Disability (YLD) across genders (James et al., 2018).

With the advancements in neuroscience, multiple alterations have been discovered in the depressed brain compared to the brains of healthy controls. A first set of findings highlighting differences between healthy and depressed brains can be found in the literature of structural and functional connectivity. For example, reviews and meta-analyses consistently report altered functional connectivity within the default mode network (Mulders et al., 2015; Tozzi et al., 2021), amygdala-centered connections (Tang et al., 2018), and within frontoparietal control systems and neural systems supporting salience or emotion processing (Kaiser et al., 2015). Moreover, a meta-analysis from Liao et al. (2013) describes the consistent finding of decreased fractional anisotropy in the white matter connecting the prefrontal cortex with cortical and subcortical areas.

Furthermore, the depressed brain is also characterised by altered signal analyses. Information on the neural oscillations in the cerebral cortex can be obtained in a non-invasive way, for example through EEG. Using quantitative techniques, such as a fast Fourier Transform (i.e. FFT), the power of the main frequency bands can be obtained (Dumermuth & Molinari, 1987). Typically, 5 main frequency bands are distinguished: delta (1-3 Hz), theta (4-7 Hz), alpha (8-12 Hz), beta (13-30 Hz) and gamma (30-100Hz). Multiple studies reported alterations in the power spectrum of depressed patients compared to healthy controls (Olbrich & Arns, 2013; Mahato & Paul, 2019). An often recurring finding is that depressed patients show elevated absolute (Roemer et al., 1992; von Knorring, 1983**;** Grin-Yatsenko et al., 2009; Jaworska et al., 2012) and relative (John et al., 1988; Prichep & John, 1992) alpha power. In general, an elevated alpha rhythm is associated with reduced cortical activity (Goldman et al., 2002; Laufs et al., 2003). For example, Pfurtscheller et al. (1996) demonstrated elevated alpha rhythms whenever participants were not engaged in a task. Even though some studies were unable to replicate the finding of elevated alpha in depression (Knott & Lapierre, 1987) or even report reduced alpha in depression (Price et al., 2008), the observation of elevated alpha rhythms in depression appears to be quite consistent (Mahato & Paul,

2019; Olbrich & Arns, 2013). Some studies even reported a reduction in alpha power after applying antidepressants (Itil, 1983; Leuchter et al., 2017) or non-invasive brain stimulation (Alexander et al., 2019) to depressed patients. Moreover, the importance of alpha power in the depressed brain has also been proven by machine learning studies in which alpha power provided the highest classification accuracy when trying to discriminate between healthy and depressed patients (Hosseinifarda et al., 2013; Mohammedi et al., 2015; Mahato & Paul, 2019; Mahato & Paul, 2020).

On top of general increases in alpha power, also the asymmetry between alpha power in the left versus right hemisphere is typically related to depression. A large number of studies confirm an asymmetry where the left frontal hemisphere exhibits more alpha power than the right hemisphere, resulting in a hypoactive left and an hyperactive right hemisphere (Henriques & Davidson, 1991; Smit et al., 2007; Kemp et al., 2010; Jaworska et al., 2012; Cantisani et al., 2015)(But see: Gold et al., 2013; Segrave et al., 2011). Henriques and Davidson (1991) attributed this asymmetry to approach and withdrawal motivation. According to the approach-withdrawal model, the left frontal regions are mostly involved in approach-related, positive affect (Depue & Iacono, 1989; Harmon-Jones, 2003; Coan & Allen, 2004) whereas the right frontal regions are more associated with behavioural inhibition and negative affective states (Davidson & Irwin, 1999; Coan & Allen, 2004). Individual differences in frontal asymmetry would thus be underlying the affective style and by consequence the sensitivity to depression (Davidson, 1992; Davidson, 1998).

Within the frontal regions, the dorsolateral prefrontal cortex (DLPFC) plays an important role in emotion regulation through reappraisal of negative emotions (Lévesque et al., 2003; Grimm et al., 2008; Golkar et al., 2012). For example, Lévesque et al. (2003) found in their fMRI study that DLPFC showed higher activation when participants were asked to suppress their emotional response to sad stimuli than when they were allowed to react normally. Moreover, Golkar et al. (2012) found that this activity in DLPFC during reappraisal was independent of the valence of the emotional stimulus. These findings suggest an important role of DLPFC in depression, where emotion regulation is known to be dysfunctional (Gross & Muñoz, 1995; Joormann & Gotlib, 2010). Indeed, in line with the asymmetry in alpha power in the frontal regions of depressed patients, such an asymmetry in activity in the DLPFC has also been

demonstrated using fMRI (Baxter et al., 1989; Bench et al., 1993; Grimm et al., 2008). For example, Grimm et al. (2008) found with their fMRI study that MDD patients showed hypoactivity in the left DLPFC during emotional judgement. Moreover, in contrast to the left DLPFC, the right DLPFC has been found to be hyperactive during emotional judgement (Grimm et al., 2008) which is consistent with the finding of increased increased alpha asymmetry in depressed patients.

Despite their popularity, findings with regard to the alpha band have to be interpreted with some caution. Specifically, since the borders of the most commonly used frequency bands are artificial, averaging across such an entire band for all subjects might filter out more subtle inter-individual differences (Haegens et al., 2014). For instance, it has been shown that the alpha rhythm operates across a wider frequency range than the usually adopted range of 8-12Hz (Haegens et al., 2014). Therefore, it has been argued that a more optimal way to study alpha modulation is to obtain the individual alpha frequency (IAF) for each subject (Doppelmayr et al., 1998; Klimesch, 1999). The IAF has been studied in a wide range of contexts and has been found to correlate significantly with memory performance (Klimesch et al., 1990; Lebedev, 1994), reaction times (Surwillo, 1961; Surwillo, 1964), general intelligence (Mundy-Castle & Nelson, 1960, Grandy et al., 2013a), verbal abilities (Anokhin & Vogel, 1996) and working memory (Clark et al., 2004). Although IAF is found to be a stable neurophysiological trait marker in healthy adults (Grandy et al., 2013b), it has also been found to decrease following the manifestation of neurological disorders (Mosmans et al., 1983; Van der Worp et al., 1991; Klimesch, 1999; Luijtelaar et al., 2010; Sarnthein et al., 2006) whereas treatments can result in an increase of the IAF again (Vriens et al., 2000; Sarnthein et al., 2006). Research looking at the IAF in MDD is scarce and the conclusions are not uniform. For instance, Tement and colleagues (2016) reported a significant correlation between IAF and depression scale scores whereas Jiang and colleagues (2016) did not find a significant difference between IAF in healthy versus depressed participants.

Besides looking at the power spectrum of neural oscillations, researchers can also make use of mathematical values in the frequency domain to analyse functional connectivity. An example of such a measure is coherence (Bowyer, 2016). Coherence represents the degree of similarity between neural patterns from oscillating brain

activity, taking both frequency and amplitude into account (Shaw, 1981; Hughes & John, 1999; Srinivasan et al., 2007; Bowyer, 2016; Youh et al., 2017; Basharpoor et al., 2019). It reflects the consistency of the relative phase and amplitude between the signals, detected through electrodes, within a given frequency band (Bowyer, 2016). Coherence can take values from 0 to 1, where a value of 1 indicates that the compared signals are identical (Boywer, 2016; Srinivasan et al., 2007). In reality however, coherence is very sensitive to the distortions in the brain signals obtained through EEG or MEG because of a conduction problem (Srinivasan et al., 2007). Therefore, alternative measures can also be used to mathematically measure functional connectivity between two neural signals. One example is the phase-locking value (PLV), which only describes the difference in phase between two signals and is thus not influenced by fluctuations in amplitudes (Lachaux et al., 1999; Mormann et al., 2000; Aydore et al., 2013). Another alternative measure is the phase lag index (PLI), which quantifies the asymmetry of the relative phase distribution around zero and thus only reports high values when the relative phase exhibits a peak away from zero (Aydore et al., 2013).

Although the literature on coherence in depression is not very extensive and some studies report reduced coherence in depressed patients versus healthy controls (Knott et al., 2001; Suhhova et al., 2009), others demonstrated increases in coherence within the alpha band in depressed patients (Leuchter et al., 2012; Petchkovsky et al., 2013; Li et al., 2016; Markovska-Simoska et al., 2018). Moreover, Petchkovsky et al. (2013) reported a decrease in this hypercoherence after administration of choir therapy to patients with depression. In addition, studies using other measures of phase synchronization also reported increased functional connectivity within the alpha band in depressed patients (Olbrich et al., 2014; Hasanzadeh et al., 2018; Zhang et al., 2020).

A final distinction between healthy and depressed brains can be described in terms of the excitatory/inhibitory (E/I) balance in the brain. Specifically, the depressed brain is characterised by inhibitory deficits (Croarkin et al., 2011). The balance between excitation and inhibition in neural circuits is essential to maintain normal brain functioning (He & Cline, 2019). When the E/I-balance is impaired, this can give rise to brain dysfunctions which can be found in certain neurological disorders (He & Cline, 2019), such as MDD (Levinson et al., 2010). Numerous studies reported a reduction in

GABA neurons, which are responsible for inhibitory transmission (Levinson et al., 2010; Croarkin et al., 2011). Specifically, Rajkowska et al. (2017) demonstrated a reduction in both size and density of GABA neurons in the DLPFC of patients suffering from MDD. Moreover, Sibell et al. (2011) and Schür et al. (2016) provided evidence for a reduction of GABA in this same region. In addition, a trend towards reduced GABA was also demonstrated in the dorsolateral prefrontal cortex (Rajkowska et al., 2017). Finally, multiple authors noted decreased GABA in the occipital cortex of depressed patients (Maciag et al., 2010; Schür et al., 2016; Sanacora et al., 2002; Sanacora et al., 2004; Hughes et al., 2011). Importantly, this reduction in GABA in the occipital cortex is no longer found in patients in remission (Schür et al., 2016) and the amount of GABA in this region has been found to increase after treating patients with serotonin reuptake inhibitors (Sanacora et al., 2002) or electroconvulsive therapy (Sanacora et al., 2003).

Non-invasive brain stimulation

Despite advancements in pharmacology, 20-30% of patients cannot be treated with medication or psychotherapy and thus belong to the category of treatment-resistant depression (TRD). When these treatments fail to improve the patients symptoms, one can turn to the use of neuromodulation techniques. These techniques can be divided in three different categories. There are (1) seizure therapies, such as electroconvulsive therapy (ECT) and magnetic seizure therapy (MST), (2) neurosurgical therapies such as vagus nerve stimulation (VNS), electroconvulsive therapy (ECS) and deep brain stimulation (DBS) and (3) noninvasive therapies like transcranial magnetic stimulation (TMS**)**, transcranial direct current stimulation (TDCS) and cranial electrotherapy stimulation (CES)(Al-Harbi & Qureshi, 2012). In their meta-analysis, Al-Harbi and Qureshi (2012) found that 30-93% of TRD patients experienced significant improvements after treatments with one of these techniques. One big advantage of these techniques is that, in contrast to pharmacological treatments, these techniques only affect a small part of the body, thus possibly reducing general side-effects. However, not all side-effects can be excluded. For example, ECT is known to be an efficient treatment for TRD (Kellner et al., 2012) but is also associated with relatively many cognitive side effects (Rami-Gonzalez et al., 2001). Although neurosurgical therapies have proven to be very efficient, the downside of these techniques is that they are very invasive. Therefore, a lot of researchers currently focus on the third group, namely the

noninvasive neuromodulation techniques, which also show a good efficiency, are not as invasive as the neurosurgical therapies and are associated with far less side-effects than seizure therapies (Al-Harbi & Qureshi, 2012).

These noninvasive neurostimulation techniques make use of magnetic fields ore electric currents to stimulate specific brain areas (Carpenter, 2006; Cusin & Peyda, 2019). Some of them have already shown promising results for diminishing the symptoms of patients with TRD (Al-Harbi & Qureshi, 2012). One commonly used non-invasive neurostimulation technique is TMS (transcranial magnetic stimulation). This technique uses a coil in which electric pulses are generated which in turn induce a magnetic field under the coil (Barker et al., 1985). When the coil is placed on the skull, this magnetic field causes an electric field that is capable of depolarizing local neurons to a depth of 2cm under the skull (Barker et al., 1985; Lefaucheur et al., 2014). When such TMS pulses are sent repetitively (i.e., repetitive TMS [rTMS]), the effects of the stimulation persist longer (Lefaucher et al., 2014). A wide range of studies using rTMS to target the left dorsolateral prefrontal cortex (DLPFC) have already shown significant reductions in depressive symptoms in MDD (Brunelin, et al., 2007; Fitzgerald et al., 2006; Holtzheimer et al., 2001; Martin et al., 2003; Teng et al., 2017).

As mentioned before, a region which plays a significant role in MDD is the DLPFC. This functional region is located in the prefrontal cortex in the middle frontal gyrus and consists of Brodmann's areas 9 and 46 (Brodmann, 1909). Because it is not a deep structure, it can be targeted using non-invasive neuromodulation techniques. Different types of rTMS protocols aim at either increasing activity in the hypoactive left DLPFC or decreasing activity in the hyperactive right DLPFC (Yadollahpour et al., 2016). Low frequency rTMS (LF-rTMS), with a frequency < 1Hz, is generally applied to the hyperactive DLPFC because of its inhibitory effects (Hoffman & Cavus., 2002; Yadollahpour et al., 2016).On the other hand, high frequency rTMS (HF-rTMS), often with a frequency > 10Hz (Yadollahpour et al., 2016), is known to induce excitatory effects and therefore often targeted to the hypoactive left DLPFC (Maeda et al., 2000; Yadollahpour et al., 2016). By such applications of rTMS, researchers aim to restore the imbalance between the left and right DLPFC in depressed patients (Fitzgerald et al., 2003; Isenberg et al., 2005; Leuchter et al., 2013). Although both protocols have been proven successful in treating symptoms of MDD (Isenberg et al., 2005; Fitzgerald et al.,

2009; Cao et al., 2018), Valiulis and colleagues (2012) demonstrated that both rTMS protocols strongly differ in their electrophysiological mechanisms. Specifically, Valiulis and colleagues (2012) reported an effect of LF-rTMS on the alpha band whereas the HF-rTMS protocol was found to induce wider electrophysiological changes in the brain. One way to inspect the effect of rTMS on brain signals, is by virtually simulating it through TVB.

Current study

In the current study we made use of the Wilson-Cowan model implemented in TVB to simulate four groups of brain types: 1) healthy brain, 2) depressed brain, 3) depressed brain with HF-rTMS and 4) depressed brain with LF-rTMS. For each of the types 100 unique virtual brain signals were obtained by altering the noise seed for each simulation. Based on the literature reporting reduced inhibition in the DLPFC, orbitofrontal and occipital cortex of depressed patients, the Q-parameter in the Wilson-Cowan model was reduced in the depressed brains compared to the healthy brains in the aforementioned regions. HF-rTMS was applied with a frequency of 10Hz to the left DLPFC whereas a frequency of 1Hz targeting the right DLFPC was used to simulate the depressed brain with LF-rTMS. Next, the brain activity of the four brain types was compared in terms of power spectrum and functional connectivity. Given the fact that we worked with simulations and thus had no issues with conduction, we used coherence as a measure for functional connectivity. Moreover, because looking at an entire power band with its fixed artificial boundaries might filter out more subtle differences, we decided to also look at the individual alpha peak (IAF) of each simulated brain. In addition, measures of power spectrum and coherence were each repeated five times: across the entire alpha band (8-12Hz) and across four subbands (8-9Hz, 9-10Hz, 10-11Hz, 11-12Hz) since, although not very common practice, looking at subranges of the alpha band can also be done to avoid averaging out more subtle differences (Klimesch et al., 1998). Specifically, we wanted to see whether a) healthy and depressed brains show the expected differences in alpha power, IAF and coherence, b) stimulation of the depressed brains can cause the resulting brain activity to shift more towards a healthy activity, and c) if so, which stimulation type results in the best improvements. Given the literature, we expected to find an increased alpha power as well as an increased frontal

alpha asymmetry and increased coherence in the baseline depressed brain (without stimulation) compared to the healthy brain. Moreover, we expected these differences in the depressed brain to return to 'normal' after both HF-rTMS and LF-rTMS. Specially: we thus expected that the depressed brain with HF-TMS or LF-rTMS would no longer significantly differ from the healthy brain in terms of power spectrum and functional connectivity.

Method

Materials

All simulations were performed on the default connectivity matrix using the tvb-library (version 2.2; Sanz-Leon et al., 2013) in Jupyter notebooks running on Python 2.7.9 (Kluyver et al., 2016). After extracting the resulting local field potentials, analyses of the power spectrum and coherence were performed with help of the following Python packages: numpy (Harris et al., 2020), scipy (Virtanen et al., 2020), FOOOF (Haller et al., 2018), matplotlib (Hunter, 2007) and pandas (McKinney, 2010). Analyses on the peak in alpha power were conducted using R studio (R Core Team, 2019) with lme4 (Bates et al., 2015), emmeans (Length, 2020) and car (Fox and Weisberg, 2019). The significance level was set at $p = 0.05$ (two-tailed) for all analyses. All simulations and analyses were performed on a HP Pavilion (Intel core i7, 8 GB RAM)

Simulating virtual brains

In total, we simulated four different brain types using the Wilson-Cowan model: 1) healthy virtual brains, 2) depressed virtual brains, 3) depressed brains with HF-rTMS and 4) depressed brains with LF-rTMS. For each brain type, 2.5s of local field potentials for 100 unique subjects were simulated by adjusting the noise seed for each simulation. Thus, in total 400 brains were simulated using Jupyter notebooks.

Healthy brain. First, the interactive phase plane in the GUI of TVB was explored to obtain the optimal parameters of the Wilson-Cowan model to generate realistic oscillatory behaviour (figure 4A). An overview of the used parameters can be found in appendix A. Once the optimal parameters were obtained, additive noise was implemented in the model using a stochastic integrator. Default values were used for all

additional simulation parameters. These parameters were then used to simulate the set of healthy brains and were later used as the basis for the other simulated brain types.

Depressed brain. In the following step, we created the set of depressed brains by adapting the amount of inhibition in the DLPFC, orbitofrontal and occipital cortex in both hemispheres. This was achieved by reducing the Q parameter to its minimum value (0). As can be seen in figure 4B, this resulted in less inhibition while still showing realistic oscillations. In all the other regions of the depressed brain, the same set of parameter values as in the healthy brain simulation was used.

Figure 4

Phase plane of the Wilson-Cowan model

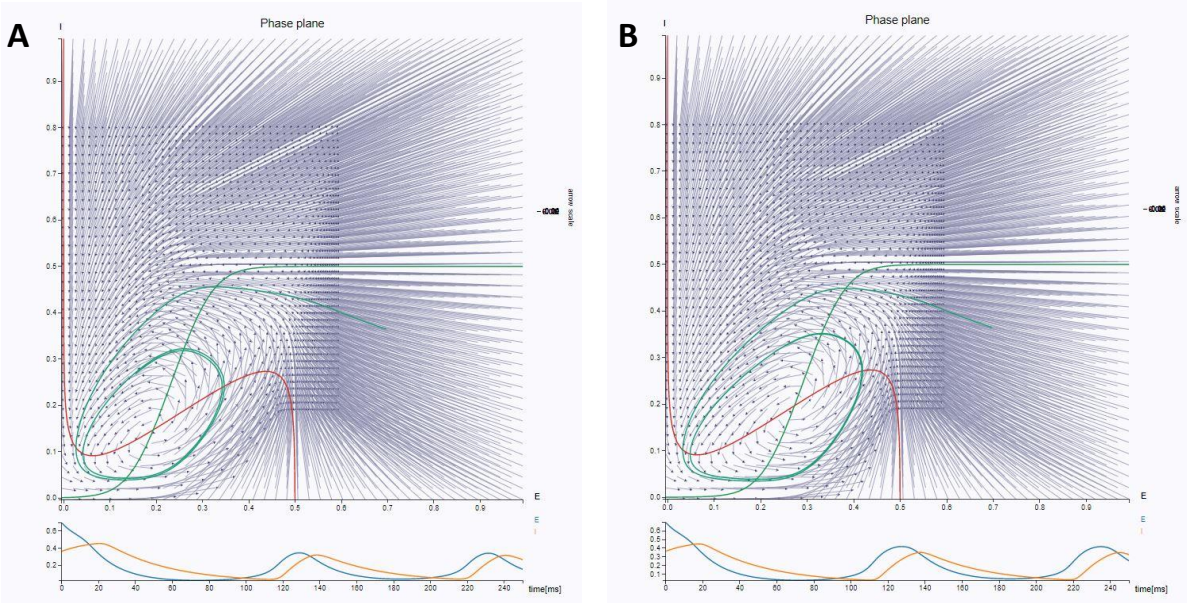

Note. Phase planes based on state variables I and E of the Wilson-Cowan model with our chosen parameters, obtained through the GUI of TVB. In both figures a limit cycle is reached. A) Represents the healthy parameters. Used to model the entire healthy brain and the regions of the depressed brain where the inhibition parameter was not reduced. B) Represents the model with less inhbiition (reduced Q). Used in the DLPFC, orbitofrontal cortex and occipital cortex in the depressed brain.

Depressed brain with HF-rTMS. Next, a region stimulus was created to mimic HF-rTMS. We used a pulsetrain with an immediate onset and a 100ms inter-stimulus-

interval, resulting in a 10Hz stimulation (figure 5). The amplitude was kept similar to the amplitude of the healthy and depressed brain signals to make sure the stimulation would not completely dominate the resulting brain signals. To model the effects of HF-rTMS, new simulations were made with the same model parameters as the baseline depressed brain but this time with addition of the high frequency stimuli to the left DLPFC, with a scaling factor of 5.

Depressed brain with LF-rTMS. To simulate the effects of LF-rTMS, new simulations were again created with the same parameter values as the baseline depressed brain. This time, low frequency stimuli were applied to the right DLPFC with a scaling factor of 5. The only difference with the high frequency stimulation was that in the low frequency stimulation a 1000ms inter-stimulus interval was used, resulting in 1Hz stimulation (figure 5).

Figure 5

rTMS stimuli

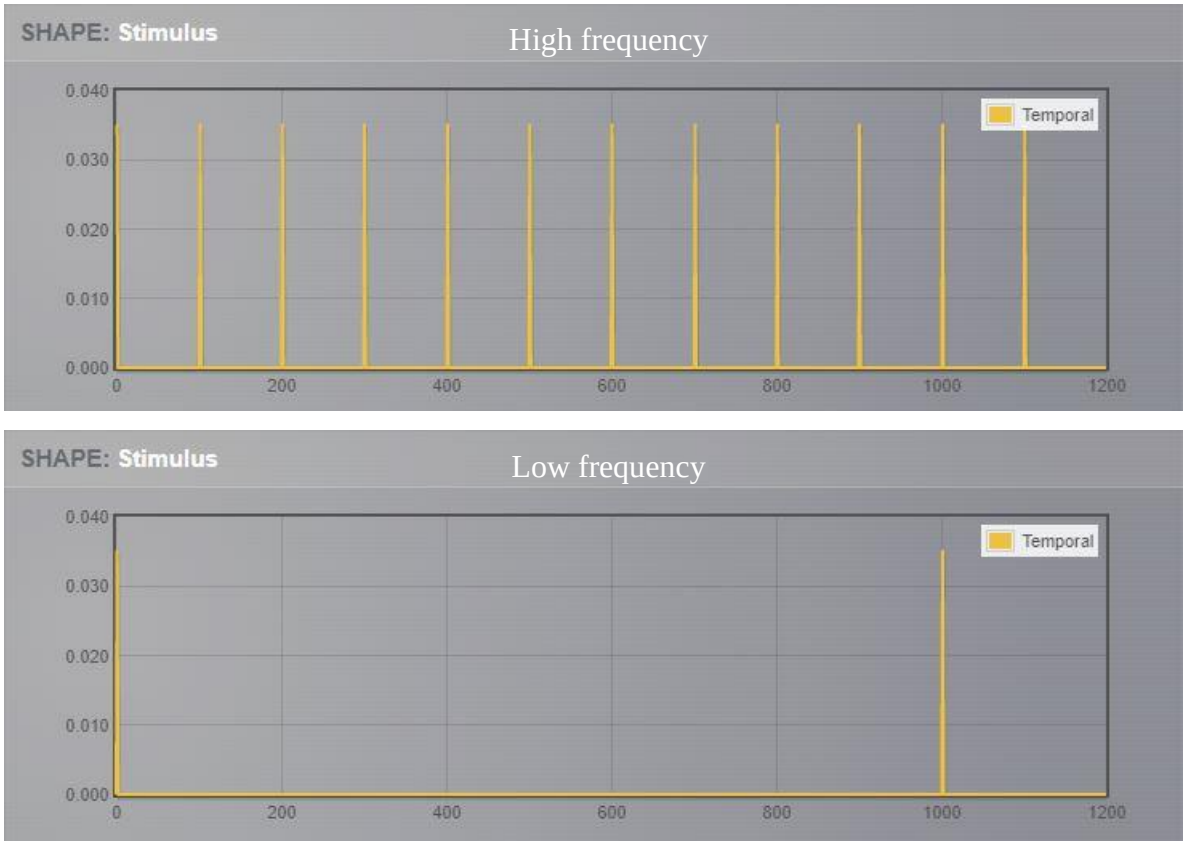

Note. Images created in the GUI of TVB. Both images show stimuli applied within a time window of 1.2 seconds. Time in ms is displayed on the x-axis whereas the y-axis

represents the amplitude of the stimuli. Top figure: High frequency rTMS with a frequency of 10Hz. Bottom figure: Low frequency rTMS with a frequency of 1Hz.

Data analyses

The first step before any of the analyses was to delete the first 500ms of the local field potentials from each brain simulation. This was done because the system needs time to reach a steady state (i.e., limit cycle in the phase plane) which can induce artefacts in the data.

For all outcome measures, 6 comparisons were made: 1) Healthy versus Depressed, 2) Healthy versus LF-rTMS, 3) Healthy versus HF-rTMS, 4) Depressed versus LF-rTMS, 5) Depressed versus HF-rTMS, 6) LF-rTMS versus HF-rTMS. Comparisons 4 and 5 can be seen as pre- versus post-treatment results where the depressed brain serves as the baseline depressed brain before treatment and the LF-rTMS and HF-rTMS brains are that same brain after receiving treatment in the form of rTMS. Making all of these comparisons allows us to see whether there are baseline differences between the healthy and the depressed brain and which changes both protocols of rTMS induce compared to these baseline brains. Moreover, comparison 6 allows for comparison between the two treatment protocols.

Given the importance of frontal, temporal, occipital and parietal cortical regions in literature regarding coherence (Leuchter et al., 2012; Li et al., 2016), 28 ROIs (i.e. regions of interest) were included in our study. Specifically, frontal eye fields (FEF), inferior parietal cortex (PCI), medial parietal cortex (PCM), superior parietal cortex (PCS), centrolateral prefrontal cortex (PFCCL), dorsolateral prefrontal cortex (PFCDL), dorsomedial prefrontal cortex (PFCDM), medial prefrontal cortex (PFCM), orbitofrontal cortex (PFCORB), central temporal cortex (TCC), superior temporal cortex (TCS), inferior temporal cortex (TCI), primary visual cortex (V1) and secondary visual cortex (V2) were included bilaterally in our analyses of coherence as well as in the analyses of the peak in alpha power.

Alpha power. Analyses on alpha power were focused on the DLPFC, given its importance in depression. Alpha power (8-12Hz) was measured by first obtaining the power spectrum of each individual simulation (n = 400) using Welch's method (Welch, 1967), which consisted of a fast Fourier Transform (FFT) with a Hann window. This

yielded alpha power in $\mu V^2/Hz$. Absolute alpha power in both left and right DLPFC was then computed by approximating the area under the curve across the entire alpha band (8-12Hz) and across four subbands (8-9Hz, 9-10Hz, 10-11Hz, 11-12Hz). In a next step, frontal alpha asymmetry was obtained as left frontal alpha power (lDLPFC) divided by right frontal alpha power (rDLPFC). Positive outcomes thus represented higher alpha power in the left compared to the right DLPFC. T-tests were performed in Python to compare alpha power across all groups and the Holm-Bonferroni method was used to correct for multiple comparisons (Holm, 1979). Moreover, Cohen's d was calculated as a measure of effect sizes.

Alpha peak. Because fixed pre-defined frequency ranges are artificial and might miss out on more subtle changes, we decided to also extract the peak within the alpha frequency (8-12Hz) from each simulated brain. To do so, the FOOOF package was used (Haller et al., 2018). The advantage of this package is that it allows users to obtain the center frequency of the peak as well as the power while also controlling for the aperiodic component. In our analyses, we used power^2 as a proxy for amplitude. For each of the 400 simulated brains, the peak in alpha power was extracted for each of the 28 included ROIs, resulting in 11200 extracted peaks. In 0.5% of the fittings, the model was unable to find a fit and thus no information on the peak could be extracted. Specifically, model fitting was unsuccessful for 16 simulations in the rV1, 32 simulations in the lPFCDL and 16 simulations in the rV2. Analyses of the peaks were performed in R (R Core Team, 2019) using the linear mixed effects model framework. In separate analyses, center frequency of the peak and amplitude of the peak were used as outcome measures. For both analyses, *Group* (healthy, depressed, HF-rTMS, LF-rTMS) and *ROI* (28 included ROIs) were included as predictors. A random intercept across subjects (each individual simulated brain) was included in all models. In the post-hoc analyses, the Tukey method was used to correct for multiple comparisons.

Coherence. Coherence was calculated across the entire alpha band between all 28 included ROIs, resulting in 378 region comparisons for each of the 400 simulated brains. These calculations were repeated for each of the four alpha subbands. T-tests were used to test the differences between the four brain types in terms of coherence. Again, the Holm-Bonferroni correction was applied to correct for multiple comparisons (Holm, 1979). Finally, Cohen's d was obtained as an indication for the effect sizes.

Code accessibility

All code used for this paper is freely available on https://github.com/CelienI/TVB_project

Results

Frontal alpha power

Differences in alpha power were examined across the entire alpha band (8-12Hz) and within four subbands (8-9Hz, 9-10Hz, 10-11Hz, 11-12Hz) for both right and left DLPFC.

Left frontal alpha (lDLPFC). When looking across the entire alpha band (8-12Hz) we found evidence for a significantly increased alpha power in the depressed versus the healthy brains in the left DLPFC, in line with our expectations ($t(199) = 161.52$, $p < 0.001$, $d = 22.84$)(figure 6; appendix B). However, no evidence was found for treatment effects of either of the rTMS protocols. Specifically, differences in left frontal alpha power between healthy brains and the depressed brains after both HF-rTMS and LF-rTMS remained significant (all t's >2.67, all p's < 0.02, all d's > 0.38). Moreover, HF-rTMS induced an even higher increase in alpha power compared to the baseline depressed brain ($t(199) = 29.48$, $p < 0.001$, d's = 4.17). The same pattern of increased left frontal alpha power in depressed versus healthy brains (all t's > 7.55, all p's < 0.001, all d's > 1.07), increased alpha in both rTMS protocols compared to healthy brains (all t's > 6.33, all p's < 0.001, all d's > 0.89) and increased alpha in HF-rTMS as compared to baseline depressed brains (all t's > 11.08, all p's < 0.001, all d's > 1.57) was found in the two lowest alpha subbands (8-9Hz, 9-10Hz). In contrast, in the 10-11Hz subband alpha power was higher in the healthy brains compared to the depressed brains ($t(199) = 18.13$, $p < 0.001$, $d = 2.56$). With the exception of the unsignificant differences in alpha power within this subband between the depressed and LF-rTMS groups ($t(199) = 0.03$, $p = 1.00$, $d = 0.00$), all other group comparisons within this subband were significant (all t's > 2.98, all p's < 0.001, all d's > 0.28) with alpha power being highest in healthy brains and lowest in depressed and LF-rTMS brains. Finally, no significant difference between the healthy and depressed group were found in terms of left frontal alpha power in the highest subband ($t(199) = 0.42$, $p = 0.67$, $d = 0.06$). Within this subband, the only significant group comparisons were those of each group

compared to the HF-rTMS group (all *t*'s > 5.64, all *p*'s < 0.001, all *d*'s > 0.80) where the HF-rTMS resulted in the highest alpha power.

Right frontal alpha (rDLPFC). Across the entire alpha band and the two lowest subbands, alpha power was again significantly higher in the depressed group as compared to the healthy group (all *t*'s > 9.44, all *p*'s < 0.001, all *d*'s > 1.34)(appendix C). In the two remaining subbands alpha power was significantly lower in the depressed group compared to the healthy group (all *t*'s > 4.35, all *p*'s < 0.001, all *d*'s > 0.62). HF-rTMS did not induce any significant differences in right frontal alpha power compared to the baseline depressed group in any of the subbands nor across the entire band (all *t*'s < 0.06, all *p*'s = 1.00, all *d*'s < 0.01). Both the HF-rTMS group and the LF-rTMS group significantly differed from the healthy group across all (sub)bands (all *t*'s > 4.38, all *p*'s < 0.001, all *d*'s > 0.62) where the healthy group had a significantly higher alpha power in the two highest subbands whereas alpha power was significantly lower in the healthy brain in the two lowest subbands and across the entire alpha band. Finally, LF-rTMS resulted in significantly higher right frontal alpha power compared to baseline depressed and HF-rTMS brains in all frequency (sub)bands (all *t*'s >21.02, all *p*'s < 0.001, all *d*'s > 0.74) except for the 9-10Hz band (all *t*'s < 12.37, all *p*'s > 0.23, all *d*'s < 0.17).

Frontal asymmetry. Frontal asymmetry was measured as the ratio of alpha power in the left compared to the right DLPFC where a positive ratio thus indicates a higher level of alpha power in the left DLPFC. In contrast to our expectations, we found evidence for a significantly higher left frontal asymmetry in the healthy group compared to the depressed group across the entire alpha band ($t(199) = 3.69$, $p = 0.001$, $d = 0.52$) and within the 9-10Hz subband ($t(199) = 3.30$, $p = 0.003$, $d = 0.47$)(appendix D). Across the entire alpha band and the 9-10Hz subband all other group comparisons were significant as well (all *t*'s > 6.72, all *p*'s < 0.001, all *d*'s > 0.95) with the LF-rTMS group exhibiting the highest left frontal asymmetry, followed by lower asymmetry in the healthy and depressed brains and the lowest asymmetry in the HF-rTMS group. Furthermore, within the 10-11Hz subband we found evidence for a significantly increased frontal alpha asymmetry in the depressed versus healthy group ($t(199) = 4.22$, $p = 0.003$, $d = 0.47$). Except for the non-significant comparison between the baseline depressed and the LF-rTMS group ($t(199) = 1.69$, $p = 0.093$, $d = 0.24$), all other comparisons within this subband were significant (all *t*'s > 3.28, all *p*'s < 0.001, all *d*'s

> 0.46) with the highest asymmetry being found in the HF-rTMS group and the lowest in the healthy group. Within the remaining subbands, no baseline difference in frontal asymmetry was revealed between the healthy and depressed groups (all *t*'s < 0.32, all *p*'s = 1.00, all *d*'s < 0.05). However, all other group comparisons within these subbands were significant (all *t*'s > 3.15, all *p*'s < 0.006, all *d*'s > 0.48) with highest asymmetry in the HF-rTMS group and lowest asymmetry in the LF-rTMS group.

Figure 6

Alpha power in DLPFC

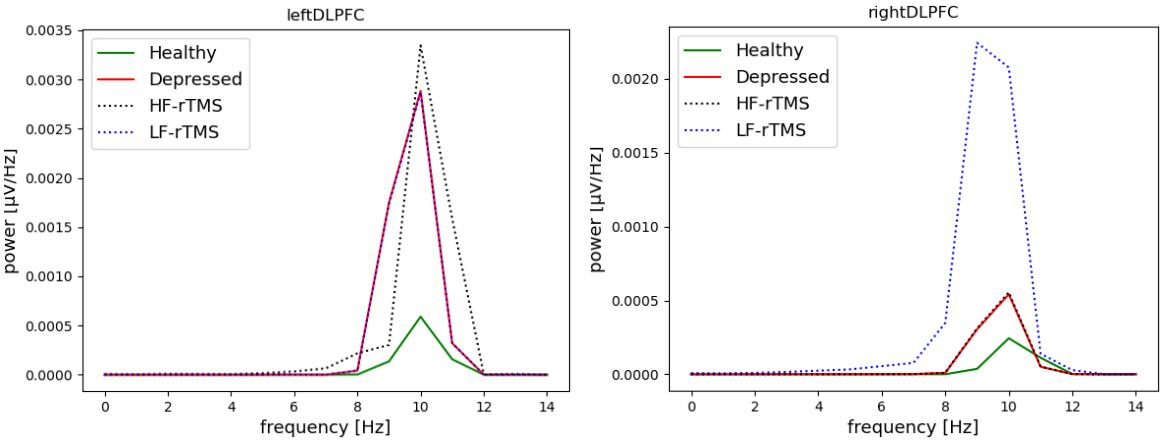

Note. Power across the entire alpha band (8-12Hz). Frequencies are shown on the x-axis whereas power spectral density is represented by the y-axis. The left figure plots the alpha power in the left DLPFC (on average per group) whereas the right figure plots this same information for the right DLPFC.

Alpha peak

Peak frequency. Analyses of the peak frequency revealed a significant interaction between *Group* and *ROI* (χ2(81, 2784) = 2279.33, *p* < 0.001). When further examining this interaction, it was found that there were no significant group differences in peak frequency within the following regions: lFEF, lPCI, lPCM, lPCS, lPFCCL, lPFCDM, lPFCM, lTCI, lTCS, rFEF, rPCI, rPCM, rPCS, rPFCCl, rPFCDM, rPFCM, rTCC, rTCS (all *z*'s < 1.86, all *p*'s > 0.245). However, in both hemispheres the peak frequency in the depressed brains significantly differed from the peak frequency in the healthy brains in PFCDL, PFCORB, V1 and V2 (all *z*'s > 3.14, all *p*'s < 0.009) where

the peak in the depressed brain happened at a lower frequency compared to the healthy peak (figure 7). In lPFCDL, LF-rTMS did not result in a significant shift in peak compared to the baseline depressed peak (z = 0.038, p = 1.00). All other group comparisons in this region were found to be significant (all z's > 3.142, all p's < 0.009). Specifically, the peak happened at the lowest frequency for the depressed and LF-rTMS brain, at a significantly higher frequency in the healthy brain and again at a significantly higher frequency in the HF-rTMS group. In the right counterpart of this region (rPFCDL) as well as in left and right PFCORB, V1 and V2, none of the rTMS protocols led to a significant shift in peak frequency compared to the baseline depressed brain (all z's < 0.74, all p's > 0.880). Indeed, in none of these regions a significant shift in peak was found in the HF-rTMS brains compared to the LF-rTMS brains (all z's < 0.74, all p's > 0.880). All other comparisons in these regions were significant (all z's > 14.72, all p's < 0.001), where the peak in the healthy brains was consistently found at a higher frequency compared to the other groups.

Peak amplitude. For the amplitude of the peak in alpha power, another significant interaction was found between *Group* and *ROI* (χ2(81, 2784) = 291.33, p < 0.001). Further analyses revealed no significant differences between any of the groups in the following regions: lFEF, lPCI, lPCM, lPCS, lPFCCL, lPFCDM, lPFCM, lTCC, lTCI, lTCS, lV1, lV2, rFEF, rPCI, rPCM, rPCS, rPFCCL, rPFCDM, rPFCM, rTCC, rTCI, rTCS, rV1, rV2 (all z's < 0.98, all p's > 0.670)(figure 7). In the lPFCDL, no significant difference was found between healthy, depressed and LF-rTMS (all z's < 0.69, all p's > 0.901) whereas the remaining comparisons were significant (all z's > 8.39, all p's < 0.001). Specifically, the peak amplitude was significantly lower in the HF-rTMS brains compared to the other groups. In both left and right PFCORB, a significant difference was revealed between the depressed and the healthy brains as well as between the HF-rTMS and the healthy brains (all z's > 3.20, all p's < 0.008). Specifically, the healthy brains were found to have the lowest peak amplitude. In the left PFCORB, the comparison between LF-rTMS and healthy brains also revealed a significant difference in peak amplitude where the amplitude of the healthy brains still remained the lowest. Other comparisons in the left and right PFCORB were not significant (all z's < 2.48, all p's > 0.064). Finally, in rPFCDL the LF-rTMS brains showed a significantly lower peak amplitude compared to the other groups (all z's >

7.51, all p's < 0.001) whereas the other comparisons revealed no significant differences (all z's < 0.53, all p's > 0.952).

Figure 7

Frequency and power of the peak in alpha power

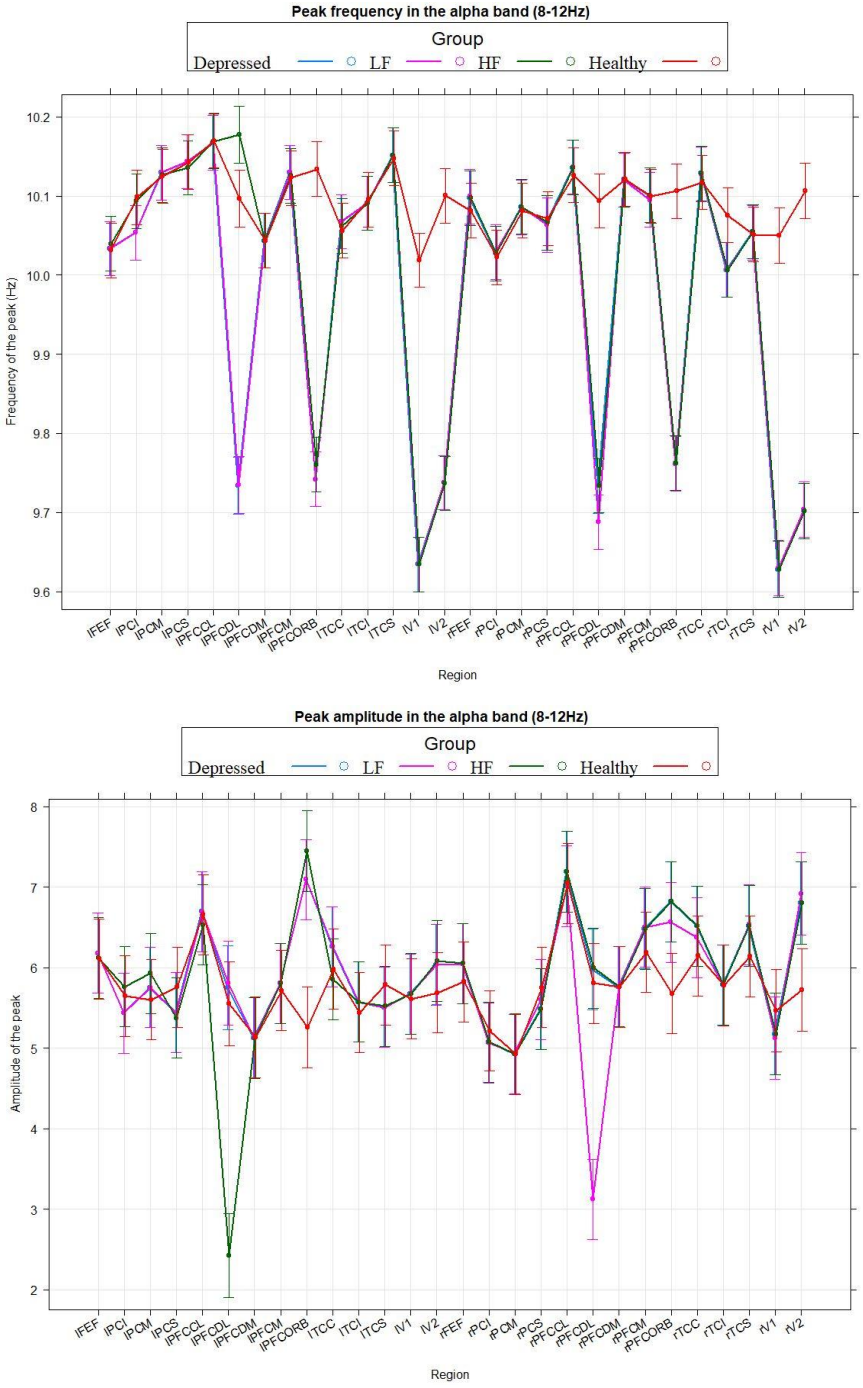

Note. Top figure shows the centre frequency of the extracted peak in alpha power for each of the included ROIs. Bottom figure shows the amplitude of the extracted peak in alpha power for each of the included ROIs. Error bars are based on a 95% confidence interval.

Coherence

Coherence between all included regions was calculated in each of the alpha subbands (8-9Hz, 9-10Hz, 10-11Hz, 11-12Hz) and across the entire alpha band at once (8-12Hz).

Across the entire alpha band, coherence in the healthy group was significantly lower compared to the three other groups between rPCS and lV1 (all $t > 4.75$, all p's < 0.001, d's > 0.20), between rV22 and lPFCM (all t's > 4.46, all p's < 0.003, d's > 0.19) and between rTCS and lV1 (all t's > 4.35, all p's < 0.003, all d's > 0.19). Within these regions, no significant differences were found between the depressed, HF-rTMS and LF-rTMS groups (all t's < 0.43, all p's $= 1.00$, all d's < 0.02) (figure 8). Furthermore, when comparing rFEF with rPFCDL, no significant differences were found (all t's < 2.90, all p's $= 1.00$, all d's < 0.12) except between the healthy and LF-rTMS groups ($t(199) = 5.07$, $p < 0.001$, $d = 0.22$), where LF-rTMS resulted in a significantly higher coherence (figure 8). Next, a significantly lower coherence between rPFCDL and lPFCM was found in the LF-rTMS group compared to the depressed and the HF-rTMS groups (all t's > 4.02, all p's < 0.022, all d's > 0.17). Other comparisons between these regions were not significant (all t's < 2.69, all p's $= 1.00$, all d's < 0.11). Lastly, a significantly higher coherence between lPFC and lPFCDL and between lFEF and lPFCDL in the HF-rTMS group compared to the depressed group (all t's > 4.36, all p's < 0.004, all d's > 0.19) whereas a significantly lower coherence between rPFCM and lPFCDL and between rFEF and lPFCDL in the HF-rTMS was found compared to the depressed group (all t's > 3.85, all p's < 0.045, all d's > 0.16). All other comparisons were not significant (all t's < 3.64, all p's > 0.055, all d's < 0.15).

Within the lowest alpha band (8-9Hz), the coherence of the healthy group was significantly higher compared to the depressed group in the rPCS-lFEF, rPCS-lV1, rPCS-lPFCCL and the rPFCDM-rV2 (all t's > 3.89, all p's < 0.048, all d's > 0.32). In contrast, coherence of the healthy group was significantly lower compared to the

depressed group within rPFCDL-lPFCM, rV1-lPCM, rTCS-lV1, rPFCORB-lV1, rV1-lTCI and lTCC-lV2 (all t's > 3.98, all p's < 0.029, all d's > 0.33). Furthermore, the healthy group was found to have a significantly higher coherence within rPCS-lFEF and rPCS-lV1 compared to the LF-rTMS group and the HF-rTMS group (all t's > 4.40, all p's < 0.005, all d's > 0.36) whereas coherence of the healthy group was significantly lower compared to both rTMS groups within rTCS-lV1, rPFCORB-lV1 and rV1-lTCI (all t's > 3.76, all p's < 0.028 , all d's > 0.29). When comparing the healthy group with the LF-rTMS group, significantly lower coherence in the healthy group was revealed within rV1-lPCM, rPCS-rTCS and lTCC-lV2 (all t's > 3.98, all p's < 0.029, all d's > 0.32) whereas coherence in the healthy group was significantly lower between rTCC-rTCI ($t(199) = 3.85$, $p = 0.048$, $d = 0.31$). Furthermore, HF-rTMS resulted in significantly higher coherence compared to the healthy group in lPCS-lPFCDL, lPFCDL-lPFCM, rPFCDL-lPCM and rPFCORB-lTCC whereas this type of stimulation resulted in significantly lower coherence compared to the healthy group in lPCI-lV2, rTCC-lPFCORB and rPFCDM, rV2 (all t's > 3.88, all p's < 0.041 , all d's > 0.32). Within rPFCM-lPFCDL and rPCM-lPFCDL, a significantly lower coherence was found for the HF-rTMS group compared to the LF-rTMs and baseline depression group (all t's > 4.92, all p's < 0.001, all d's > 0.40). Finally, LF-rTMS resulted in a significantly lower coherence between rPFCDL and rPFCORB compared to the depressed group and the HF-rTMS group (all t's > 4.27, all p's < 0.004, all d's > 0.35). All other comparisons were not significant (all t's < 3.61, all p's > 0.10, all d's < 0.29).

Within the 9-10Hz subband, coherence between lPCI and lPFCORB as well as between rFEF and lV1 was significantly higher in the healthy compared to the depressed, LF-rTMS and HF-rTMS groups (all t's > 4.11, all p's < 0.002 , all d's < 0.41). Coherence between lPCS and lPFCDL was significantly higher in the healthy and the HF-rTMS groups compared to the depressed and LF-rTMS groups (all t's > 5.20, all p's < 0.001, all d's > 0.52). Next, coherence in the healthy group between rTCI and lV1 was significantly lower compared to the three other groups (all t's > 4.60, all p's < 0.001, all d's > 0.46) whereas it was significantly higher in the healthy group compared to the depressed and HF-rTMS group between rTCI and lV1 (all t's > 3.96, all p's < 0.032, all d's > 0.40). Between rV2 and lPFCM, coherence was significantly higher in the healthy group compared to the depressed and LF-rTMS groups (all t's > 3.95, all p's

< 0.035, al *d*'s > 0.39). Furthermore, a significant increase in coherence between lPCM and lPCS was found in the HF-rTMS compared to the heatlhy group ($t(199) = 4.42$, $p = 0.004$, $d = 0.44$). Finally, HF-rTMS resulted in significantly increase coherence between rV2 and lPFCDL compared to the depressed and LF-rTMS groups (all *t*'s > 4.24; all *p*'s < 0.011; all *d*'s > 0.42). All other comparisons were not significant (all *t*'s < 3.84, all *p*'s > 0.053, all *d*'s < 0.38).

In the 10-11Hz subband, coherence between lPFCDL and LPFCORB was significantly higher in the healthy and HF-rTMS groups compared to the depressed and LF-rTMS groups (all *t*'s > 6.49, all *p*'s < 0.001, all *d*'s > 0.53). Between rPFCORB and lPFCDM, coherence was significantly higher in the healthy group compared to the other groups (all *t*'s > 4.13, all *p*'s < 0.016, all *d*'s > 0.34). In contrast, coherence in the healthy group was lower compared to the depressed and HF-rTMS groups between rPCI and lV1 (all *t*'s > 4.02, all *p*'s < 0.025, all *d*'s > 0.33). Furthermore, HF-rTMS led to a significant increase in coherence compared to the other groups between lFEF and lPFCDL (all *t*'s > 4.19, all *p*'s < 0.012, all *d*'s > 0.34). Finally, HF-rTMS was found to have a significantly higher coherence compared to the LF-rTMS and depressed group between lPCS and lPFCDL (all *t*'s > 4.18, all *p*'s < 0.012, all *d*'s > 0.34). All other comparisons did not reach significance (all *t*'s < 4.04, all *p*'s > 0.077, all *d*'s < 0.31).

Lastly, within the 11-12Hz subband, coherence between lPFCCl and lPFCDL was found to be significantly lower in the HF-rTMS group compared to the other groups (all *t*'s > 4.85, all *p*'s < 0.001, all *d*'s > 0.40). A significiantly lower coherence in the HF-rTMS group compared to the healthy group was also found between the lPCM and lPFCDL regions ($t(199) = 4.20$, $p = 0.011$, $d = 0.34$). Finally, coherence between lPFCDL and lTCC was significantly higher in the HF-rTMS group compared to the depressed and LF-rTMS groups (all *t*'s > 4.12, all *p*'s < 0.016, all *d*'s >0.34). No further significant comparisons were found (all *t*'s < 3.76, all *p*'s > 0.071, all *d*'s < 0.31).

Figure 8

Coherence between included ROIs

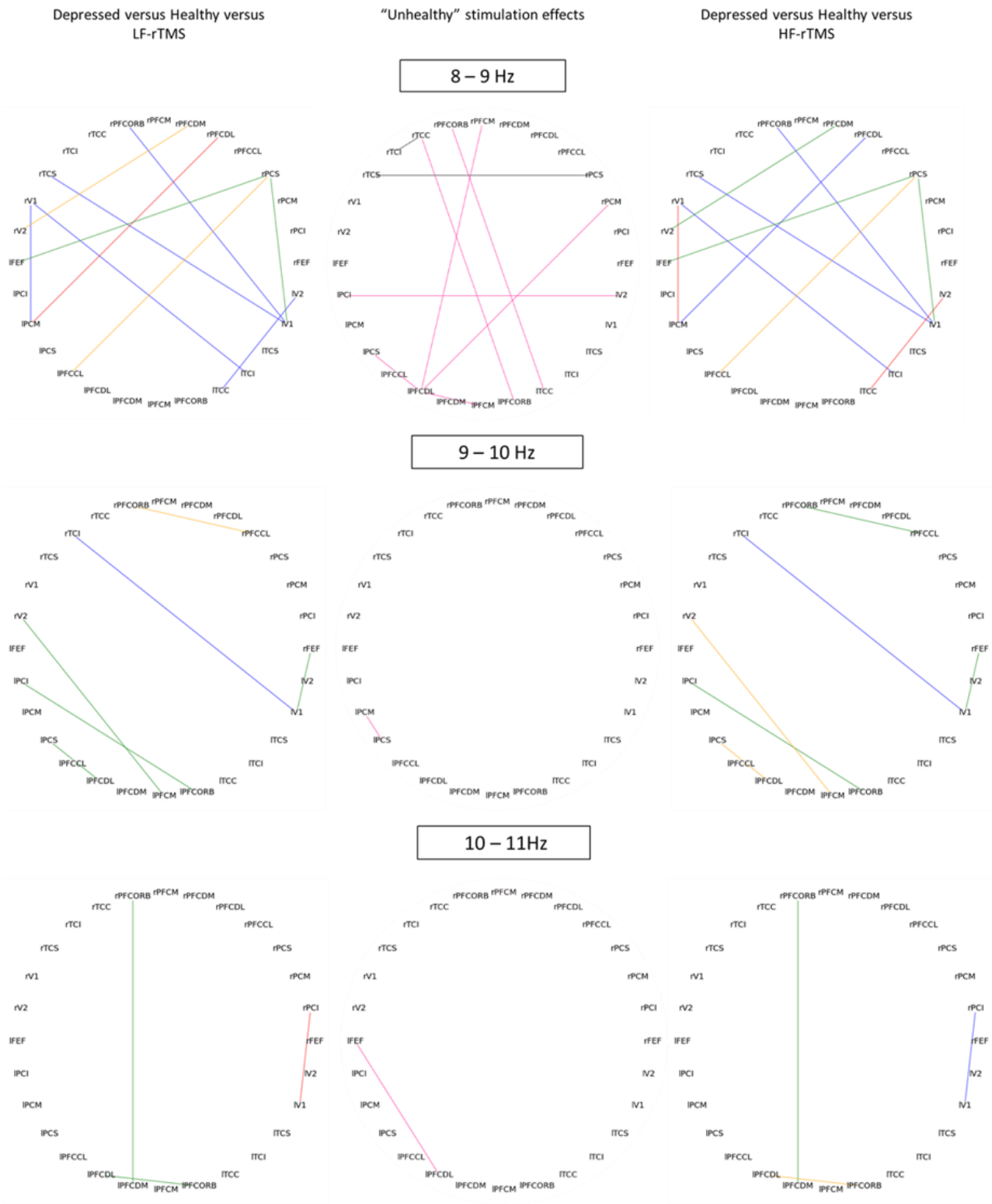

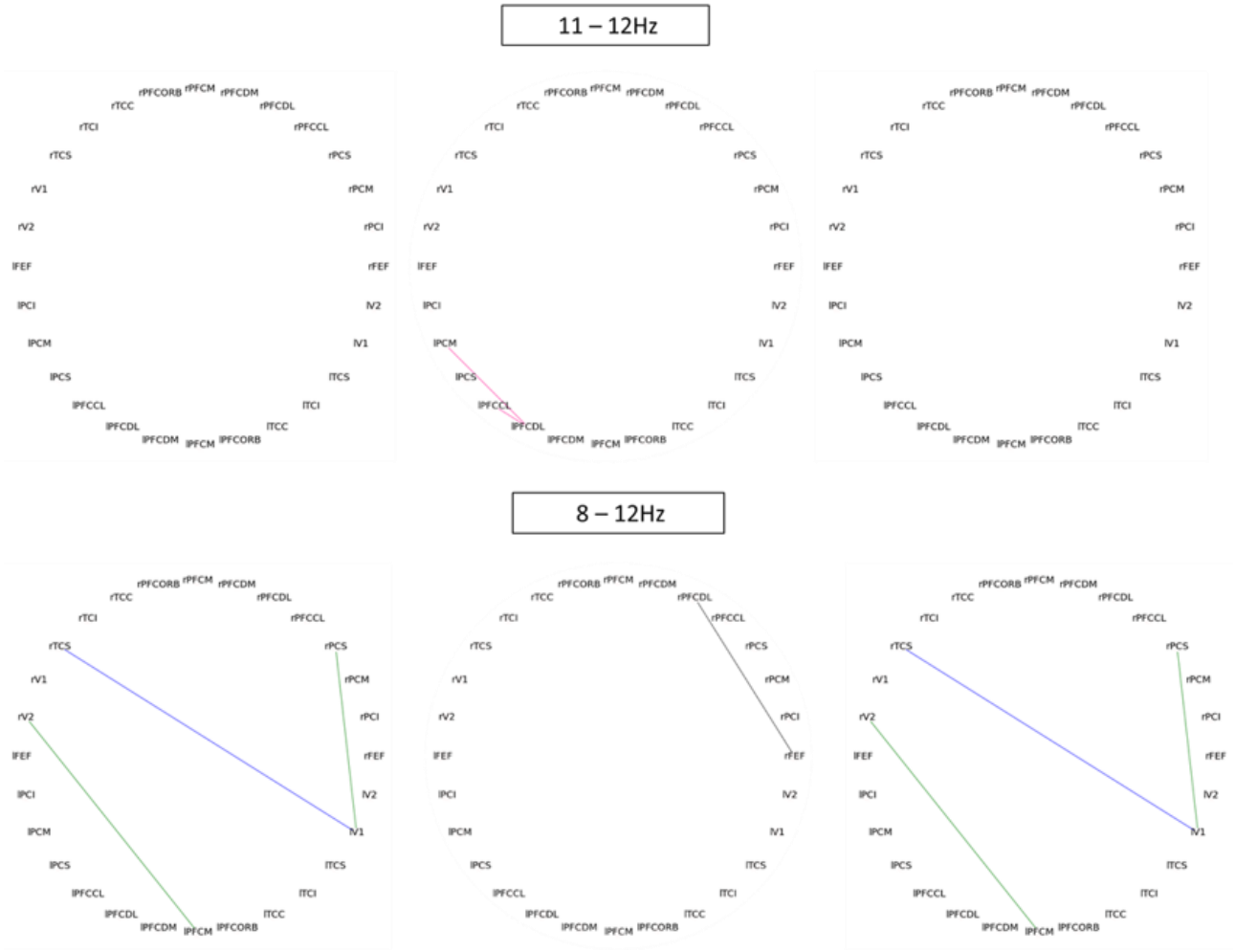

Note. Each of the 28 included ROIs is represented in a circular network where connections between regions (full lines) represent significant coherence changes between groups. Each row of graphs represents a different frequency (sub)band. Graphs in the left column represent significant differences between healthy and depressed brains compared to LF-rTMS whereas the graphs in the right column represent the differences between healthy, depressed and HF-rTMS brains. In these graphs, blue lines indicate a significantly higher coherence in depressed versus healthy brains without normalization towards healthy values after stimulation. Red lines also indicate an increased coherence in depressed versus healthy brains where the coherence of the depressed brain after stimulation was no longer significantly different from the healthy

brain. Green lines show an increased coherence in healthy compared to depressed brains where coherence of the depressed brain after stimulation still remains significantly different compared to the healthy brains whereas in yellow lines, the depressed brain coherence was no longer significantly different from the healthy brain after stimulation. The middle column of graphs represents 'unhealthy' stimulation effects. Specifically, lines indicate region pairs where coherence was not significantly different between healthy and depressed brains but the depressed brain became significantly different from the healthy brain after HF-rTMS (black), LF-rTMS (purple) or both stimulation protocols (light blue).

Discussion

Frontal alpha power

Our results regarding left frontal alpha power across the entire alpha band are in line with our expectations. Namely, we found evidence for a significant increase in alpha power in depressed versus healthy subjects. This same evidence was found for the two lowest subbands of alpha power. However, no treatment effects were revealed in these (sub)bands. Specifically, LF-rTMS did not induce any significant differences between the baseline depressed brain and the depressed brain after LF-rTMS. Moreover, instead of reducing the increased alpha power in depression, HF-rTMS resulted in an even bigger increase in alpha power. In addition, our results were not unambiguous. Specifically, no difference in left frontal alpha power between the healthy and depressed groups was found within the 11-12Hz subband whereas the difference between these groups pointed toward a significantly decreased left frontal alpha power in the depressed group within the 10-11Hz subband. Remarkably, within the 10-11Hz subband HF-rTMS seemed to again enlarge the already existing difference between the healthy and baseline depressed groups, this time by resulting in the lowest amount of frontal alpha power.

Across the entire alpha band as well as in the two lowest subbands we found evidence for an increased right frontal alpha power in the depressed versus the healthy group. In the two highest subbands this effect was reversed. The HF-rTMS group did not significantly differ from the baseline depressed group in any of the (sub)bands. However, LF-rTMS did induce significant differences in the depressed brains in all (sub)bands except within the 9-10Hz subband.

In contrast to our expectations we found evidence for a significantly higher left frontal asymmetry in the healthy group as compared to the depressed group across the entire alpha band and within the 9-10Hz subband. Within these frequency bands LF-rTMS resulted in the highest left frontal asymmetry whereas HF-rTMS resulted in a frontal asymmetry in which right alpha power was higher than left frontal alpha power. However, in the 10-11Hz subband we did find evidence for an increased asymmetry in depressed versus healthy subjects, which is in line with our expectations. In the last subband (11-12Hz), no significant differences between healthy and depressed brains were found. Finally, no treatment-like effects were found for either LF-rTMS nor HF-rTMS.

Although our results in terms of increased frontal alpha power were in line with our expectations across the entire alpha band, we did find some inconsistencies across subbands. First of all, comparison to literature is not straightforward given the existing inconsistencies across studies. For example, though some reviews conclude that alpha power is indeed increased in depressed brains (Olbrich & Arns, 2013; Mahato & Paul, 2019), others researchers reported a decrease in alpha power in depressed patients (Flor-Henry, 1979; Price et al., 2008; Kan & Lee, 2015; Jiang et al., 2016). In addition, the review of de Aguiar Neta and Rosa (2019) concluded that the alpha band power is not a reliable diagnostic marker of depression. Possibly, the variability in methods used to assess alpha power in depression can be an explanation for the mixed results in literature. For instance, many studies only look at alpha power across the entire alpha band, which might miss out on more subtle differences in subbands of the alpha band. Due to the lack of studies using multiple subbands, we cannot directly compare our results from the subbands to literature. As for the entire alpha band, the range of frequencies is only artificial and not all researchers use the same frequency boundaries. The range is often chosen from 8Hz to 12Hz but multiple authors also used a lower boundary of 7.5Hz and/or an upper boundary of 13Hz (Kemp et al., 2010; Jaworska et al., 2012; Cantisani et al., 2015). The danger of these artificially fixed power bands is that too narrow bands might miss significant portions of alpha power that fall outside of the fixed window whereas too wide ranges might erroneously include neighbouring frequencies in the alpha window (Klimesch et al., 1996; Klimesch et al., 1998). Definitely given the fact that some researchers report significant changes in power in

these neighbouring theta and beta bands in depressed patients at frontal sites (Knott et al., 2001; Begić et al., 2011), including these frequencies in the alpha band could cause faulty conclusions on the amount of alpha power.

With regard to left frontal asymmetry we only found evidence in line with our expectations within the 10-11Hz subband. In contrast, the results across the entire alpha band were at odds with our hypotheses. However, we are not the first failing to replicate the general finding of increased left frontal asymmetry in depressed patients (Segrave et al., 2011; Gold et al., 2013). Moreover, although most studies who reported an increased asymmetry in depressed patients did not look at subbands (e.g., Henriques & Davidson, 1991; Smit et al., 2007; Kemp et al., 2010), the findings of studies who did are inconsistent. For instance, both Jaworska et al. (2012) and Cantisani et al. (2015) looked at the entire alpha band, lower alpha band and higher alpha band. Remarkably, Cantisani et al. (2015) reported increased asymmetry across the entire alpha band and the two subbands whereas Jaworska et al. (2012) only found this asymmetry in the upper alpha band (10.5-13Hz).

Again, some reviews and meta-analyses doubt the importance of alpha asymmetry as a diagnostic marker for depression (Van Der Vinne et al., 2017; de Aguiar Neto & Rosa, 2019). It is proposed that alpha asymmetry is more useful in predicting specific symptoms and treatment outcome (Van Der Vinne et al., 2017; Nelson et al., 2018) rather than as a diagnostic marker. The major reason for this proposal is the inconsistency in literature on frontal alpha asymmetry. Some authors propose these inconsistencies might be caused by an underlying impact of gender in alpha asymmetry (Bruder et al., 2017; de Aguiar Neto & Rosa, 2019). However, authors failing to find gender impact on alpha asymmetry (Smith et al., 2018) cause doubts about this idea.

Both of the stimulation protocols could not induce any treatment-like effects in our data. In general, results revealed strong effects of HF-rTMS in the left DLPFC where HF-rTMS enlarged the already existing differences between healthy and baseline depressed brains. In contrast, LF-rTMS had this same effect in the right DLPFC. Also in terms of frontal asymmetry, none of the stimulation protocols resulted in an amount of asymmetry that was closer to the healthy values than to the baseline depressed values.

Alpha peak

For the individual alpha peak (IAF), no significant differences between the four brain types were found for most of the included ROIs. With regards to the peak frequency of the IAF, a significantly lower peak frequency was revealed in the depressed group compared to the healthy group within the bilateral PFCDL, PFCORB, V1 and V2. No differences between the peak frequencies in the depressed group were found compared to any of the stimulation groups in bilateral PFCORB, V1, V2 and right DLPFC. However, in left DLPFC HF-rTMS resulted in a significantly higher peak frequency as compared to the baseline depressed brain, thus inducing a treatment-like effect. Although shifting the peak frequency into the right direction, the effect of HF-rTMS seems a bit too strong since the resulting peak frequency is also significantly higher than the healthy brain (figure 7).

For the amplitude of the IAF, the amplitude of the peak was found to be significantly lower in the healthy brains whereas no significant differences were found between the amplitudes of the peaks in the depressed brains, HF-rTMS brains and LF-rTMS brains. However, in right PFCORB, LF-rTMS resulted in a shift towards a lower amplitude which was no longer significantly different from the healthy brain (figure 7), thus causing a treatment-effect. In addition, in left DLPFC HF-rTMS resulted in a significantly lower peak amplitude as compared to the other groups whereas in right DLPFC LF-rTMS resulted in a significantly lower amplitude.

Taken together, the IAF only revealed significant differences between the healthy and depressed brains in frontal and occipital regions in terms of peak frequency and only in frontal regions in terms of peak amplitude. Literature on IAF in depression is scarce and results are mixed. For instance, Tement and colleagues (2016) found a significant correlation between IAF and depression scores whereas Jiang and colleagues (2016) did not find a significant difference between IAF in healthy versus depressed patients. However, in both of these studies IAF was calculated based on the average power spectrum of a set of frontal EEG-electrodes which makes comparison to our results, calculated for individual regions, harder. Although scarce, we did find some evidence that HF-rTMS and LF-rTMS are able to cause treatment-like shifts in peak frequency and/or amplitude.

Coherence

In line with existing literature, our results on coherence were diverse. We found evidence for both increased and decreased coherence in depression compared to healthy brains. Moreover, for many region comparisons, no significant differences were found. Our results differed across frequency (sub)bands (figure 8). For instance, the amount of significant region pairs in terms of differences in coherence between healthy and depressed brains differed across (sub)bands, where most significant pairs were found in the lowest subband (8-9Hz) whereas no significant pairs were revealed in the highest subband (11-12Hz). In addition, around half of the significant pairs in the lowest alpha band revealed a significantly higher coherence in depression as compared to healthy brains whereas the other half represented a significantly lower coherence in depression. In other (sub)bands, there was an overweight of significant pairs representing significantly lower coherence in depression. Finally, in the three lowest subbands, we found evidence of treatment effects of LF-rTMS or HF-rTMS in a little more than half of the region pairs showing a significantly different coherence between healthy and baseline depression brains (figure 8). In contrast, coherence values of depressed brains did not return to 'healthy' values after any type of stimulation when looking across the entire alpha band (8-12Hz).

Remarkably, we did notice some region pairs for which there was no difference in coherence between the baseline depressed brains and the healthy brains but where either HF-rTMS or LF-rTMS induced shifts in coherence that became significantly different from the healthy brains (figure 8). The effects of both rTMS protocols were thus not limited to the regions showing an altered coherence in baseline depressed brains.

Finally, in terms of effects on coherence we seem to have found evidence that the underlying mechanisms of HF-rTMS and LF-rTMS are not identical. Specifically, whereas coherence of some region pairs was significantly changed by one type of rTMS, none of the region pairs were significantly changed by both protocols.

Again, comparison with literature is not an easy job given the scarcity of studies looking at coherence in depression. Moreover, some studies only compare a few region pairs (e.g., Knott et al., 2001; Suhhova et al., 2009; Markovska-Simoska et al., 2018) whereas others compare all possible regions acquired with EEG (Leuchter et al. 2012). In addition, in these studies the lower boundary of the measured alpha power ranges

from 7.5Hz to 8Hz whereas the upper boundary ranges from 12Hz to 13Hz across the aforementioned studies which could again lead to too many or too little frequencies included as 'alpha' across studies. Moreover, our inconsistent findings across subbands highlight the effects of choosing different frequency range boundaries on the results.

General discussion

In general, our results were not unambiguously in line with our predictions. Looking across the entire alpha band we found evidence for an increase in frontal alpha power in depressed versus healthy brains. However, within subbands there were inconsistent results. Moreover, we could not find evidence for an increased left frontal asymmetry in depressed brains versus healthy brains across the entire alpha band. Furthermore, depending on the region comparison we found both evidence for increased, decreased and unchanged coherence in depressed versus healthy brains. Finally, although we found some evidence for treatment-like effects in IAF and coherence of some region pairs, in general our indications of treatment effects of both rTMS protocols were scarce.

One possible explanation for the lack of results in line with our predictions on differences in depressed versus healthy brains and the lack of treatment-like effects could be that our model was not successful at mimicking depressed brains. Based on literature, we lowered the Q parameter of the Wilson-Cowan model in specific regions in the depressed brains. However, alterations in depressed brains are widespread in both structural (e.g., Liao et al., 2013) and functional connectivity (e.g., Kaiser et al., 2015) as well as in neurotransmitters (e.g., Nutt, 2008; Pan et al., 2018). Therefore, altering the amount of inhibition alone might not be enough to mimic a typical depressed brain. In addition, we extracted local field potentials from virtual brains while they were being stimulated with either HF-rTMS or LF-rTMS. In real patient studies however, EEG and/or behavioural measures are collected after the rTMS treatment instead of during. Perhaps we missed out on more treatment-like effects because it takes some time before the effects of rTMS become clear.

An alternative approach which might lead to more reliable results would be to use the individual data of real depressed and control subjects. A model could then be fitted for each brain individually and will probably capture the real differences between

the healthy and depressed brains in a more realistic way. Unfortunately, we did not have such data available which is why we chose to work with one default brain and alter the model parameters based on literature.

Furthermore, we only simulated 2.5s of brain activity for each individual brain of which the first 500ms were deleted to prevent artefacts. This short simulation period was chosen due to the lack of great computational power. However, it might make comparison with results from real patient-studies more difficult since real patient-studies record data over longer periods of time. On the other hand, the 2s of brain activity we simulated could be used entirely since, in contrast to real patient data, we did not have to delete artefacts caused by eyeblinks and movements.

However, even with a perfect model for healthy and depressed brains and even with longer simulation times, comparing our results to literature is not a straightforward job given the inconsistencies. For instance, Thibodeau and colleagues (2016) report that part of the variability in effect sizes across studies regarding frontal asymmetry can be contributed to differences in depression operationalization and length of resting EEG data. Moreover, Van Der Vinne and colleagues (2017) did not find evidence for frontal asymmetry in depression with their meta-analysis. Moreover, they demonstrate that most studies regarding frontal asymmetry are severely underpowered. Furthermore, researchers studying IAF and/or coherence in depression are scarce and ambiguous. In addition, most studies make use of fixed alpha bands with varying upper and lower boundaries which can result in capturing too much or too little data as alpha power (Klimesch et al., 1996; Klimesch et al., 1998). Indeed, our inconsistent results across frequency subbands expose the danger of missing out on more subtle differences when averaging across an entire frequency band. Specifically, we were able to replicate the increased frontal alpha power in depressed brains across the entire alpha band but also found evidence in the opposite direction when inspecting some of the subbands. These issues expose the need for more (uniform) research within the domain of depression.

Conclusion

In conclusion, we replicated the finding of increased frontal alpha power in depressed brains but some inconsistent results were found within the frequency subbands. In addition, we did not find evidence for an increased frontal alpha

asymmetry in depression. Moreover, we found evidence for both increased, decreased and equal coherence between healthy and depressed brains depending on the region pairs. Furthermore, differences in IAF between the healthy and depressed groups were only found in some frontal and occipital regions. Finally, treatment-like effects of both rTMS protocols were scarce and no evidence was found that would indicate that one of the protocols would be more superior compared to the other. Given the inconsistencies in literature, comparing our results to real patient-studies is not straightforward. Possibly, our model of the depressed brains was too simplistic. We thus argue that future research repeating our study with the data from real depressed patients instead of the default brain in TVB would yield more realistic results.

References

Ajilore, O., Lamar, M., Leow, A., Zhang, A., Yang, S., & Kumar, A. (2014). Graph theory analysis of cortical-subcortical networks in late-life depression. *The American Journal of Geriatric Psychiatry*, *22*(2), 195-206.

Alexander, M. L., Alagapan, S., Lugo, C. E., Mellin, J. M., Lustenberger, C., Rubinow, D. R., & Fröhlich, F. (2019). Double-blind, randomized pilot clinical trial targeting alpha oscillations with transcranial alternating current stimulation (tACS) for the treatment of major depressive disorder (MDD). *Translational psychiatry*, *9*(1), 1-12.

Al-Harbi, K. S., & Qureshi, N. A. (2012). Neuromodulation therapies and treatment-resistant depression. *Medical Devices* (Auckland, NZ), 5, 53.

Anokhin, A., & Vogel, F. (1996). EEG alpha rhythm frequency and intelligence in normal adults. *Intelligence*, *23*(1), 1-14.

Aydore, S., Pantazis, D., & Leahy, R. M. (2013). A note on the phase locking value and its properties. *Neuroimage*, *74*, 231-244.

Baggio, H. C., Sala-Llonch, R., Segura, B., Marti, M. J., Valldeoriola, F., Compta, Y., ... & Junqué, C. (2014). Functional brain networks and cognitive deficits in Parkinson's disease. *Human brain mapping*, *35*(9), 4620-4634.

Barker, A. T., Jalinous, R., & Freeston, I. L. (1985). Non-invasive magnetic stimulation of human motor cortex. *The Lancet*, *325*(8437), 1106-1107.

Basharpoor, S., Heidari, F., & Molavi, P. (2019). EEG coherence in theta, alpha, and beta bands in frontal regions and executive functions. *Applied Neuropsychology*: Adult, 1-8.

Baxter, L. R., Schwartz, J. M., Phelps, M. E., Mazziotta, J. C., Guze, B. H., Selin, C. E., ... & Sumida, R. M. (1989). Reduction of prefrontal cortex glucose metabolism common to three types of depression. *Archives of general psychiatry*, *46*(3), 243-250.

Begić, D., Popović-Knapić, V., Grubišin, J., Kosanović-Rajačić, B., Filipčić, I., Telarović, I., & Jakovljević, M. (2011). Quantitative electroencephalography in schizophrenia and depression. *Psychiatria Danubina*, *23*(4.), 355-362.

Bench, C. J., Friston, K. J., Brown, R. G., Frackowiak, R. S. J., & Dolan, R. J. (1993). Regional cerebral blood flow in depression measured by positron emission tomography: the relationship with clinical dimensions. *Psychological medicine*, *23*(3), 579-590.

Bowyer, S. M. (2016). Coherence a measure of the brain networks: past and present. *Neuropsychiatric Electrophysiology*, *2*(1), 1-12.

Bruder, G. E., Stewart, J. W., & McGrath, P. J. (2017). Right brain, left brain in depressive disorders: clinical and theoretical implications of behavioral, electrophysiological and neuroimaging findings. *Neuroscience & Biobehavioral Reviews*, *78*, 178-191.

Brunelin, J. (2012). Low-vs high-frequency repetitive transcranial magnetic stimulation as an add-on treatment for refractory depression. *Frontiers in psychiatry*, *3*, 13.

Brunelin, J., Poulet, E., Boeuve, C., Zeroug-Vial, H., d'Amato, T., & Saoud, M. (2007). Efficacy of repetitive transcranial magnetic stimulation (rTMS) in major depression: a review. *L'Encephale*, *33*(2), 126-134.

Bullmore, E., & Sporns, O. (2009). Complex brain networks: graph theoretical analysis of structural and functional systems. *Nature reviews neuroscience*, *10*(3), 186-198.

Cantisani, A., Koenig, T., Horn, H., Müller, T., Strik, W., & Walther, S. (2015). Psychomotor retardation is linked to frontal alpha asymmetry in major depression. *Journal of affective disorders*, 188, 167-172.

Cao, X., Deng, C., Su, X., & Guo, Y. (2018). Response and remission rates following high-frequency vs. low-frequency repetitive transcranial magnetic stimulation (rTMS) over right DLPFC for treating major depressive disorder (MDD): a meta-analysis of randomized, double-blind trials. *Frontiers in psychiatry*, *9*, 413.

Carpenter, L. L. (2006). Neurostimulation in resistant depression. *Journal of Psychopharmacology*, *20*(3_suppl), 35-40.

Chadefaux, T. (2015). The triggers of war: Disentangling the spark from the powder keg. *Available at SSRN 2409005*.

Clark, C. R., Veltmeyer, M. D., Hamilton, R. J., Simms, E., Paul, R., Hermens, D., & Gordon, E. (2004). Spontaneous alpha peak frequency predicts working memory performance across the age span. *International journal of psychophysiology*, *53*(1), 1-9.

Coan, J. A., & Allen, J. J. (2004). Frontal EEG asymmetry as a moderator and mediator of emotion. *Biological psychology*, *67*(1-2), 7-50.

Croarkin, P. E., Levinson, A. J., & Daskalakis, Z. J. (2011). Evidence for GABAergic inhibitory deficits in major depressive disorder. *Neuroscience & Biobehavioral Reviews*, *35*(3), 818-825.

Cusin, C., & Peyda, S. (2019). Treatment-resistant depression. In The Massachusetts General Hospital Guide to Depression (pp. 3-19). Humana Press, Cham.

Daffertshofer, A., & van Wijk, B. (2011). On the influence of amplitude on the connectivity between phases. Frontiers in neuroinformatics, 5, 6.

Davidson, R. J. (1992). Anterior cerebral asymmetry and the nature of emotion. *Brain and cognition*, *20*(1), 125-151.

Davidson, R. J. (1998). Affective style and affective disorders: Perspectives from affective neuroscience. *Cognition & Emotion*, *12*(3), 307-330.

Davidson, R. J., & Irwin, W. (1999). The functional neuroanatomy of emotion and affective style. *Trends in cognitive sciences*, *3*(1), 11-21.

de Aguiar Neto, F. S., & Rosa, J. L. G. (2019). Depression biomarkers using non-invasive EEG: A review. *Neuroscience & Biobehavioral Reviews*, *105*, 83-93.

Depue, R. A., & Iacono, W. G. (1989). Neurobehavioral aspects of affective disorders. *Annual review of psychology*, *40*(1), 457-492.

Doppelmayr, M., Klimesch, W., Pachinger, T., & Ripper, B. (1998). Individual differences in brain dynamics: important implications for the calculation of event-related band power. *Biological cybernetics*, *79*(1), 49-57.

Duchet, B., Weerasinghe, G., Cagnan, H., Brown, P., Bick, C., & Bogacz, R. (2019). Phase dependence of response curves to stimulation and their relationship: from a Wilson-Cowan model to essential tremor patient data. *bioRxiv*, 535880.

Dumermuth, G., & Molinari, L. (1987). Spectral analysis of the EEG. *Neuropsychobiology*, *17*(1-2), 85-99.

Dwyer, D. B., Harrison, B. J., Yücel, M., Whittle, S., Zalesky, A., Pantelis, C., ... & Fornito, A. (2016). Adolescent Cognitive Control: Brain Network Dynamics. In *Stress: Concepts, Cognition, Emotion, and Behavior* (pp. 177-185). Academic Press.

Ferguson, M. A., Anderson, J. S., & Spreng, R. N. (2017). Fluid and flexible minds: Intelligence reflects synchrony in the brain's intrinsic network architecture. *Network Neuroscience*, *1*(2), 192-207.

Filippi, M., & Agosta, F. (2011). Structural and functional network connectivity breakdown in Alzheimer's disease studied with magnetic resonance imaging techniques. *Journal of Alzheimer's Disease*, *24*(3), 455-474.

Fitzgerald, P. B., Hoy, K., Daskalakis, Z. J., & Kulkarni, J. (2009). A randomized trial of the anti-depressant effects of low-and high-frequency transcranial magnetic stimulation in treatment-resistant depression. *Depression and anxiety*, *26*(3), 229-234.

Fitzgerald, P. B., Oxley, T. J., Laird, A. R., Kulkarni, J., Egan, G. F., & Daskalakis, Z. J. (2006). An analysis of functional neuroimaging studies of dorsolateral prefrontal cortical activity in depression. *Psychiatry Research: Neuroimaging*, *148*(1), 33-45.

Flor-Henry, P. (1979). Neurophysiological studies of schizophrenia, mania and depression. Hemisphere asymmetries of function in psychopathology, 182-222.

Friston, K. J. (2011). Functional and effective connectivity: a review. *Brain connectivity*, *1*(1), 13-36.

Gold, C., Fachner, J., & Erkkilä, J. (2013). Validity and reliability of electroencephalographic frontal alpha asymmetry and frontal midline theta as biomarkers for depression. *Scandinavian Journal of Psychology, 54*(2), 118-126.

Goldman, R. I., Stern, J. M., Engel Jr, J., & Cohen, M. S. (2002). Simultaneous EEG and fMRI of the alpha rhythm. *Neuroreport, 13*(18), 2487.

Golkar, A., Lonsdorf, T. B., Olsson, A., Lindstrom, K. M., Berrebi, J., Fransson, P., ... & Öhman, A. (2012). Distinct contributions of the dorsolateral prefrontal and orbitofrontal cortex during emotion regulation. *PloS one, 7*(11).

Grandy, T. H., Werkle-Bergner, M., Chicherio, C., Lövdén, M., Schmiedek, F., & Lindenberger, U. (2013a). Individual alpha peak frequency is related to latent factors of general cognitive abilities. *Neuroimage, 79*, 10-18.

Grandy, T. H., Werkle-Bergner, M., Chicherio, C., Schmiedek, F., Lövdén, M., & Lindenberger, U. (2013b). Peak individual alpha frequency qualifies as a stable neurophysiological trait marker in healthy younger and older adults. *Psychophysiology, 50*(6), 570-582.

Greicius, M. D., Flores, B. H., Menon, V., Glover, G. H., Solvason, H. B., Kenna, H., ... & Schatzberg, A. F. (2007). Resting-state functional connectivity in major depression: abnormally increased contributions from subgenual cingulate cortex and thalamus. *Biological psychiatry*, *62*(5), 429-437.

Grimm, S., Beck, J., Schuepbach, D., Hell, D., Boesiger, P., Bermpohl, F., ... & Northoff, G. (2008). Imbalance between left and right dorsolateral prefrontal cortex in major depression is linked to negative emotional judgment: an fMRI study in severe major depressive disorder. *Biological psychiatry, 63*(4), 369-376.

Grin-Yatsenko, V. A., Baas, I., Ponomarev, V. A., & Kropotov, J. D. (2009). EEG power spectra at early stages of depressive disorders. *Journal of clinical neurophysiology, 26*(6), 401-406.

Gross, J. J., & Muñoz, R. F. (1995). Emotion regulation and mental health. Clinical psychology: *Science and practice, 2*(2), 151-164.

Haegens, S., Cousijn, H., Wallis, G., Harrison, P. J., & Nobre, A. C. (2014). Inter-and intra-individual variability in alpha peak frequency. *Neuroimage, 92*, 46-55.

Haken, H. (1975). Cooperative phenomena in systems far from thermal equilibrium and in nonphysical systems. *Reviews of modern physics, 47*(1), 67.

Haller M, Donoghue T, Peterson E, Varma P, Sebastian P, Gao R, Noto T, Knight RT, Shestyuk A, Voytek B (2018) Parameterizing Neural Power Spectra. *bioRxiv, 299859*. doi: https://doi.org/10.1101/299859

Harmon-Jones, E. (2003). Anger and the behavioral approach system. Personality and Individual differences, 35(5), 995-1005.

Harris, C. R., Millman, K. J., van der Walt, S. J., Gommers, R., Virtanen, P., Cournapeau, D., … Oliphant, T. E. (2020). Array programming with NumPy. *Nature*, *585*, 357–362. https://doi.org/10.1038/s41586-020-2649-2

Hasanzadeh, F., Mohebbi, M., & Rostami, R. (2018). Investigation of functional brain networks in MDD patients based on EEG signals processing. In 2017 24th National and 2nd International Iranian Conference on Biomedical Engineering (ICBME) (pp. 1-5). IEEE.

He, H. Y., & Cline, H. T. (2019). What is excitation/inhibition and how is it regulated? A case of the elephant and the wisemen. *Journal of experimental neuroscience*, *13*, 1179069519859371.

Hearne, L. J., Mattingley, J. B., & Cocchi, L. (2016). Functional brain networks related to individual differences in human intelligence at rest. *Scientific reports*, *6*, 32328.

Henriques, Jeffrey B., and Richard J. Davidson. "Left frontal hypoactivation in depression." *Journal of abnormal psychology 100*, no. 4 (1991): 535.

Hoffman, R. E., & Cavus, I. (2002). Slow transcranial magnetic stimulation, long-term depotentiation, and brain hyperexcitability disorders. *American Journal of Psychiatry*, *159*(7), 1093-1102.

Holm, S. (1979). A simple sequentially rejective multiple test procedure. *Scandinavian journal of statistics*, 65-70.

Holtzheimer, P. 3., Russo, J., & Avery, D. H. (2001). A meta-analysis of repetitive transcranial magnetic stimulation in the treatment of depression. In Database of Abstracts of Reviews of Effects (DARE): Quality-assessed Reviews [Internet]. Centre for Reviews and Dissemination (UK).

Honey, C. J., Thivierge, J. P., & Sporns, O. (2010). Can structure predict function in the human brain?. *Neuroimage*, *52*(3), 766-776.

Hosseinifarda B, Moradia MH, Rostami R (2013) Classifying depression patients and normal subjects using machine learning techniques and nonlinear features from EEG signal. *Comput Methods Programs Biomed* 109:339–345

Hughes, J. (2011). Reduced density of calbindin immunoreactive GABAergic neurons in major depressive disorder: relevance to neuroimaging studies and future directions.

Hughes, J. R., & John, E. R. (1999). Conventional and quantitative electroencephalography in psychiatry. *The Journal of Neuropsychiatry and Clinical Neurosciences*, *11*(2), 190-208.

Hunter, J. D. (2007). Matplotlib: A 2D graphics environment. *Computing in Science & Engineering*, *9*(3), 90–95.

Isenberg, K., Downs, D., Pierce, K., Svarakic, D., Garcia, K., Jarvis, M., ... & Kormos, T. C. (2005). Low frequency rTMS stimulation of the right frontal cortex is as effective as high frequency rTMS stimulation of the left frontal cortex for antidepressant-free, treatment-resistant depressed patients. *Annals of Clinical Psychiatry*, *17*(3), 153-159.

Itil , T . (1983) . The signifi cance of quantitative pharmaco-EEG in the discovery and classifi cation of psychotropic drugs . *In W. Herrmann , (Ed.)* , Electroencephalography in Drug Research (pp. 131 – 158). Stuttgart: Gustav Fischer .

Izhikevich, E. M. (2007). *Dynamical systems in neuroscience*. MIT press.

Jacobs, H. I., Van Boxtel, M. P., Jolles, J., Verhey, F. R., & Uylings, H. B. (2012). Parietal cortex matters in Alzheimer's disease: an overview of structural, functional and metabolic findings. *Neuroscience & Biobehavioral Reviews*, *36*(1), 297-309.

James, S. L., Abate, D., Abate, K. H., Abay, S. M., Abbafati, C., Abbasi, N., ... & Abdollahpour, I. (2018). Global, regional, and national incidence, prevalence, and years lived with disability for 354 diseases and injuries for 195 countries and territories, 1990–2017: a systematic analysis for the Global Burden of Disease Study 2017. *The Lancet*, *392*(10159), 1789-1858.

Jaworska, N., Blier, P., Fusee, W., & Knott, V. (2012). Alpha power, alpha asymmetry and anterior cingulate cortex activity in depressed males and females. *Journal of psychiatric research*, *46*(11), 1483-1491.

Jiang, H., Popov, T., Jylänki, P., Bi, K., Yao, Z., Lu, Q., ... & Van Gerven, M. A. J. (2016). Predictability of depression severity based on posterior alpha oscillations. *Clinical Neurophysiology*, *127*(4), 2108-2114.

Jirsa, V., Sporns, O., Breakspear, M., Deco, G., & McIntosh, A. R. (2010). Towards the virtual brain: network modeling of the intact and the damaged brain. *Archives italiennes de biologie*, *148*(3), 189-205.

John, E. R., Prichep, L. S., Fridman, J., & Easton, P. (1988). Neurometrics: computer-assisted differential diagnosis of brain dysfunctions. *Science*, *239*(4836), 162-169.

Johnston, K. M., Powell, L. C., Anderson, I. M., Szabo, S., & Cline, S. (2019). The burden of treatment-resistant depression: a systematic review of the economic and quality of life literature. *Journal of affective disorders*, *242*, 195-210.

Joormann, J., & Gotlib, I. H. (2010). Emotion regulation in depression: Relation to cognitive inhibition. *Cognition and Emotion*, *24*(2), 281-298.

Kaiser, R. H., Andrews-Hanna, J. R., Wager, T. D., & Pizzagalli, D. A. (2015). Large-scale network dysfunction in major depressive disorder: a meta-analysis of resting-state functional connectivity. *JAMA psychiatry*, *72*(6), 603-611.

Kaiser, R. H., Whitfield-Gabrieli, S., Dillon, D. G., Goer, F., Beltzer, M., Minkel, J., ... & Pizzagalli, D. A. (2016). Dynamic resting-state functional connectivity in major depression. *Neuropsychopharmacology*, *41*(7), 1822-1830.

Kan, D. P. X., & Lee, P. F. (2015, May). Decrease alpha waves in depression: An electroencephalogram (EEG) study. In 2015 *International Conference on BioSignal Analysis, Processing and Systems (ICBAPS)* (pp. 156-161). IEEE.

Kellner, C. H., Greenberg, R. M., Murrough, J. W., Bryson, E. O., Briggs, M. C., & Pasculli, R. M. (2012). ECT in treatment-resistant depression. *American Journal of Psychiatry*, *169*(12), 1238-1244.

Kemp, A. H., Griffiths, K., Felmingham, K. L., Shankman, S. A., Drinkenburg, W. H. I. M., Arns, M., ... & Bryant, R. A. (2010). Disorder specificity despite

comorbidity: resting EEG alpha asymmetry in major depressive disorder and post-traumatic stress disorder. *Biological psychology*, *85*(2), 350-354.

Klein, E., Suchan, J., Moeller, K., Karnath, H. O., Knops, A., Wood, G., ... & Willmes, K. (2016). Considering structural connectivity in the triple code model of numerical cognition: differential connectivity for magnitude processing and arithmetic facts. *Brain Structure and Function*, *221*(2), 979-995.

Klimesch, W. (1999). EEG alpha and theta oscillations reflect cognitive and memory performance: a review and analysis. *Brain research reviews*, *29*(2-3), 169-195.

Klimesch, W., Doppelmayr, M., Russegger, H., Pachinger, T., & Schwaiger, J. (1998). Induced alpha band power changes in the human EEG and attention. *Neuroscience letters*, *244*(2), 73-76.

Klimesch, W., Doppelmayr, M., Schimke, H., & Pachinger, T. (1996). Alpha frequency, reaction time, and the speed of processing information. *Journal of clinical neurophysiology*, *13*(6), 511-518.

Klimesch, W., Schimke, H., Ladurner, G., & Pfurtscheller, G. (1990). Alpha frequency and memory performance. *Journal of Psychophysiology*.

Kluyver, T., Ragan-Kelley, B., Pérez, F., Granger, B. E., Bussonnier, M., Frederic, J., ... & et al. (2016). *Jupyter Notebooks-a publishing format for reproducible computational workflows* (Vol. 2016, pp. 87-90).

Knott, V. J., & Lapierre, Y. D. (1987). Computerized EEG correlates of depression and antidepressant treatment. *Progress in neuro-psychopharmacology & biological psychiatry*.

Knott, V., Mahoney, C., Kennedy, S., & Evans, K. (2001). EEG power, frequency, asymmetry and coherence in male depression. Psychiatry Research: *Neuroimaging*, *106*(2), 123-140.

Lachaux, J. P., Rodriguez, E., Martinerie, J., & Varela, F. J. (1999). Measuring phase synchrony in brain signals. *Human brain mapping*, *8*(4), 194-208.

Landa, P. S. (2013). *Nonlinear oscillations and waves in dynamical systems* (Vol. 360). Springer Science & Business Media.

Laufs, H., Kleinschmidt, A., Beyerle, A., Eger, E., Salek-Haddadi, A., Preibisch, C., & Krakow, K. (2003). EEG-correlated fMRI of human alpha activity. *Neuroimage*, *19*(4), 1463-1476.

Lebedev, A. N. (1994). The neurophysiological parameters of human memory. *Neuroscience and behavioral physiology, 24*(3), 254-259.

Lefaucheur, J. P., André-Obadia, N., Antal, A., Ayache, S. S., Baeken, C., Benninger, D. H., ... & Garcia-Larrea, L. (2014). Evidence-based guidelines on the therapeutic use of repetitive transcranial magnetic stimulation (rTMS). *Clinical Neurophysiology*, *125*(11), 2150-2206.

Leon, P. S., Knock, S. A., Woodman, M. M., Domide, L., Mersmann, J., McIntosh, A. R., & Jirsa, V. (2013a). The Virtual Brain: a simulator of primate brain network dynamics. *Frontiers in neuroinformatics*, *7*, 10.

Leon, P. S., Woodman, M., McIntosh, R., & Jirsa, V. (2013b). The Virtual Brain: a neuroinformatics platform for simulating large-scale brain network models. *BMC neuroscience*, *14*(S1), P193.

Leuchter, A. F., Cook, I. A., Hunter, A. M., Cai, C., & Horvath, S. (2012). Resting-state quantitative electroencephalography reveals increased neurophysiologic connectivity in depression. *PloS one*, *7*(2), e32508

Leuchter, A. F., Hunter, A. M., Jain, F. A., Tartter, M., Crump, C., & Cook, I. A. (2017). Escitalopram but not placebo modulates brain rhythmic oscillatory activity in the first week of treatment of major depressive disorder. *Journal of psychiatric research*, *84*, 174-183.

Lévesque, J., Eugene, F., Joanette, Y., Paquette, V., Mensour, B., Beaudoin, G., ... & Beauregard, M. (2003). Neural circuitry underlying voluntary suppression of sadness. *Biological psychiatry*, *53*(6), 502-510.

Levinson, A. J., Fitzgerald, P. B., Favalli, G., Blumberger, D. M., Daigle, M., & Daskalakis, Z. J. (2010). Evidence of cortical inhibitory deficits in major depressive disorder. *Biological psychiatry*, *67*(5), 458-464.

Li, Y., Kang, C., Qu, X., Zhou, Y., Wang, W., & Hu, Y. (2016). Depression-related brain connectivity analyzed by EEG event-related phase synchrony measure. *Frontiers in human neuroscience*, *10*, 477. Ook alpha

Li, Y., Liu, Y., Li, J., Qin, W., Li, K., Yu, C., & Jiang, T. (2009). Brain anatomical network and intelligence. *PLoS computational biology*, *5*(5).

Liao, Y., Huang, X., Wu, Q., Yang, C., Kuang, W., Du, M., ... & Gong, Q. (2013). Is depression a disconnection syndrome? Meta-analysis of diffusion tensor imaging

studies in patients with MDD. *Journal of psychiatry & neuroscience: JPN*, *38*(1), 49.

Liley, D. T., Alexander, D. M., Wright, J. J., & Aldous, M. D. (1999). Alpha rhythm emerges from large-scale networks of realistically coupled multicompartmental model cortical neurons. *Network: Computation in Neural Systems*, *10*(1), 79-92.

Lim, H. K., Jung, W. S., & Aizenstein, H. J. (2013). Aberrant topographical organization in gray matter structural network in late life depression: a graph theoretical analysis. *International psychogeriatrics*, *25*(12), 1929-1940.

Lo, C. Y., Wang, P. N., Chou, K. H., Wang, J., He, Y., & Lin, C. P. (2010). Diffusion tensor tractography reveals abnormal topological organization in structural cortical networks in Alzheimer's disease. *Journal of Neuroscience*, *30*(50), 16876-16885.

Long, Z., Duan, X., Wang, Y., Liu, F., Zeng, L., Zhao, J. P., & Chen, H. (2015). Disrupted structural connectivity network in treatment-naive depression. *Progress in Neuro-Psychopharmacology and Biological Psychiatry*, *56*, 18-26.

Luijtelaar, G. V., Verbraak, M., Bunt, M. V. D., Keijsers, G., & Arns, M. (2010). EEG findings in burnout patients. *The Journal of neuropsychiatry and clinical neurosciences*, *22*(2), 208-217.

Maciag, D., Hughes, J., O'Dwyer, G., Pride, Y., Stockmeier, C. A., Sanacora, G., & Rajkowska, G. (2010). Reduced density of calbindin immunoreactive GABAergic neurons in the occipital cortex in major depression: relevance to neuroimaging studies. *Biological psychiatry*, *67*(5), 465-470.

Maeda, F., Keenan, J. P., Tormos, J. M., Topka, H., & Pascual-Leone, A. (2000). Modulation of corticospinal excitability by repetitive transcranial magnetic stimulation. *Clinical neurophysiology*, *111*(5), 800-805.

Mahato, S., & Paul, S. (2019). Electroencephalogram (EEG) signal analysis for diagnosis of major depressive disorder (MDD): a review. *Nanoelectronics, Circuits and Communication Systems*, 323-335.

Mahato, S., & Paul, S. (2020). Classification of depression patients and normal subjects based on electroencephalogram (EEG) signal using alpha power and theta asymmetry. *Journal of medical systems*, *44*(1), 1-8.

Markovska-Simoska, S., Pop-Jordanova, N., & Pop-Jordanov, J. (2018). Inter-and intra-hemispheric EEG coherence study in adults with neuropsychiatric disorders. *prilozi*, *39*(2-3), 5-19

Marrelec, G., Messe, A., Giron, A., & Rudrauf, D. (2016). Functional connectivity's degenerate view of brain computation. *PLoS computational biology*, *12*(10).

Martin, J. L. R., Barbanoj, M. J., Schlaepfer, T. E., Thompson, E., Pérez, V., & Kulisevsky, J. (2003). Repetitive transcranial magnetic stimulation for the treatment of depression: systematic review and meta-analysis. *The British Journal of Psychiatry*, *182*(6), 480-491.

Maruyama, Y., Kakimoto, Y., & Araki, O. (2014). Analysis of chaotic oscillations induced in two coupled Wilson–Cowan models. *Biological cybernetics*, *108*(3), 355-363.

Matejko, A. A., Price, G. R., Mazzocco, M. M., & Ansari, D. (2013). Individual differences in left parietal white matter predict math scores on the Preliminary Scholastic Aptitude Test. *Neuroimage*, *66*, 604-610.

McKinney, W. (2010, June). Data structures for statistical computing in python. In *Proceedings of the 9th Python in Science Conference* (Vol. 445, pp. 51-56).

Mohammadi M et al (2015) Data mining EEG signals in depression for their diagnostic value. BMC Med Inf Decis Mak, pp 108–123

Mormann, F., Lehnertz, K., David, P., & Elger, C. E. (2000). Mean phase coherence as a measure for phase synchronization and its application to the EEG of epilepsy patients. *Physica D: Nonlinear Phenomena*, *144*(3-4), 358-369.

Mosmans, P. C. M., Jonkman, E. J., & Veering, M. M. (1983). CBF measured by the xenon-133 inhalation technique and quantified EEG (qEEG) investigations in patients with unilateral internal carotid artery occlusion. *Clinical neurology and neurosurgery*, *85*(3), 155-164.

Mulders, P. C., van Eijndhoven, P. F., & Beckmann, C. F. (2016). Identifying Large-Scale Neural Networks Using fMRI. In *Systems Neuroscience in Depression* (pp. 209-237). Academic Press.

Mulders, P. C., van Eijndhoven, P. F., Schene, A. H., Beckmann, C. F., & Tendolkar, I. (2015). Resting-state functional connectivity in major depressive disorder: a review. *Neuroscience & Biobehavioral Reviews*, *56*, 330-344.

Mundy-Castle, A. C., & Nelson, G. K. (1960). Intelligence, personality and brain rhythms in a socially isolated community. *Nature*, *185*(4711), 484-485.

Nelson, B. D., Kessel, E. M., Klein, D. N., & Shankman, S. A. (2018). Depression symptom dimensions and asymmetrical frontal cortical activity while anticipating reward. *Psychophysiology*, *55*(1), e12892.

Nutt, D. J. (2008). Relationship of neurotransmitters to the symptoms of major depressive disorder. *J Clin Psychiatry*, *69*(Suppl E1), 4-7.

Olbrich, S., & Arns, M. (2013). EEG biomarkers in major depressive disorder: discriminative power and prediction of treatment response. *International Review of Psychiatry*, *25*(5), 604-618.

Olbrich, S., Tränkner, A., Chittka, T., Hegerl, U., & Schönknecht, P. (2014). Functional connectivity in major depression: increased phase synchronization between frontal cortical EEG-source estimates. *Psychiatry Research: Neuroimaging*, *222*(1-2), 91-99.

Otte, C., Gold, S. M., Penninx, B. W., Pariante, C. M., Etkin, A., Fava, M., ... & Schatzberg, A. F. (2016). Major depressive disorder. *Nature reviews Disease primers*, *2*(1), 1-20.

Pan, J. X., Xia, J. J., Deng, F. L., Liang, W. W., Wu, J., Yin, B. M., ... & Xie, P. (2018). Diagnosis of major depressive disorder based on changes in multiple plasma neurotransmitters: a targeted metabolomics study. *Translational psychiatry*, *8*(1), 1-10.

Park, H. J., & Friston, K. (2013). Structural and functional brain networks: from connections to cognition. *Science*, *342*(6158), 1238411.

Peng, D. H., Ting, S. H. E. N., Zhang, J., Huang, J., Jun, L. I. U., Liu, S. Y., ... & FANG, Y. R. (2012). Abnormal functional connectivity with mood regulating circuit in unmedicated individual with major depression: a resting-state functional magnetic resonance study. *Chinese medical journal*, *125*(20), 3701-3706.

Petchkovsky, L., Robertson-Gillam, K., Kropotov, J., & Petchkovsky, M. (2013). Using QEEG parameters (asymmetry, coherence, and P3a novelty response) to track improvement in depression after choir therapy. *Advances in Mental Health*, *11*(3), 257-267.

Pfurtscheller, G., Stancak Jr, A., & Neuper, C. (1996). Event-related synchronization (ERS) in the alpha band—an electrophysiological correlate of cortical idling: a review. *International journal of psychophysiology*, *24*(1-2), 39-46.

Price, G. W., Lee, J. W., Garvey, C., & Gibson, N. (2008). Appraisal of sessional EEG features as a correlate of clinical changes in an rTMS treatment of depression. *Clinical EEG and neuroscience*, *39*(3), 131-138.

Prichep, L. S., & John, E. R. (1992). QEEG profiles of psychiatric disorders. *Brain topography*, *4*(4), 249-257.

Rajkowska, G., O'Dwyer, G., Teleki, Z., Stockmeier, C. A., & Miguel-Hidalgo, J. J. (2007). GABAergic neurons immunoreactive for calcium binding proteins are reduced in the prefrontal cortex in major depression. *Neuropsychopharmacology*, *32*(2), 471-482.

Rami-Gonzalez, L., Bernardo, M., Boget, T., Salamero, M., Gil-Verona, J. A., & Junque, C. (2001). Subtypes of memory dysfunction associated with ECT: characteristics and neurobiological bases. *The journal of ECT*, *17*(2), 129-135.

Ritchie, H., & Roser, M. (2018, 20 januari). *Mental Health*. Retrieved April 7, 2020, from https://ourworldindata.org/mental-health#citation

Ritter, P., Schirner, M., McIntosh, A. R., & Jirsa, V. K. (2013). The virtual brain integrates computational modeling and multimodal neuroimaging. *Brain connectivity*, *3*(2), 121-145.

Roemer, R. A., Shagass, C., Dubin, W., Jaffe, R., & Siegal, L. (1992). Quantitative EEG in elderly depressives. *Brain Topography*, *4*(4), 285-290

Rotarska-Jagiela, A., van de Ven, V., Oertel-Knöchel, V., Uhlhaas, P. J., Vogeley, K., & Linden, D. E. (2010). Resting-state functional network correlates of psychotic symptoms in schizophrenia. *Schizophrenia research*, *117*(1), 21-30.

Rubinov, M., & Sporns, O. (2010). Complex network measures of brain connectivity: uses and interpretations. *Neuroimage*, *52*(3), 1059-1069.

Sanacora, G., Gueorguieva, R., Epperson, C. N., Wu, Y. T., Appel, M., Rothman, D. L., ... & Mason, G. F. (2004). Subtype-specific alterations of γ-aminobutyric acid and glutamatein patients with major depression. *Archives of general psychiatry*, *61*(7), 705-713.

Sanacora, G., Mason, G. F., Rothman, D. L., & Krystal, J. H. (2002). Increased occipital cortex GABA concentrations in depressed patients after therapy with selective serotonin reuptake inhibitors. *American Journal of Psychiatry, 159*(4), 663-665.

Sanacora, G., Mason, G. F., Rothman, D. L., Hyder, F., Ciarcia, J. J., Ostroff, R. B., ... & Krystal, J. H. (2003). Increased cortical GABA concentrations in depressed patients receiving ECT. *American Journal of Psychiatry, 160*(3), 577-579.

Sanz-Leon, P., Knock, S. A., Spiegler, A., & Jirsa, V. K. (2015). Mathematical framework for large-scale brain network modeling in The Virtual Brain. *Neuroimage, 111*, 385-430.

Sanz Leon, P., Knock, S. A., Woodman, M. M., Domide, L., Mersmann, J., McIntosh, A. R., & Jirsa, V. (2013). The Virtual Brain: a simulator of primate brain network dynamics. *Frontiers in neuroinformatics, 7*, 10.

Sarnthein, J., Stern, J., Aufenberg, C., Rousson, V., & Jeanmonod, D. (2006). Increased EEG power and slowed dominant frequency in patients with neurogenic pain. *Brain, 129*(1), 55-64.

Schür, R. R., Draisma, L. W., Wijnen, J. P., Boks, M. P., Koevoets, M. G., Joëls, M., ... & Vinkers, C. H. (2016). Brain GABA levels across psychiatric disorders: A systematic literature review and meta-analysis of 1H-MRS studies. *Human brain mapping, 37*(9), 3337-3352.

Segrave, R. A., Cooper, N. R., Thomson, R. H., Croft, R. J., Sheppard, D. M., & Fitzgerald, P. B. (2011). Individualized alpha activity and frontal asymmetry in major depression. *Clinical EEG and Neuroscience, 42*(1), 45-52.

Shaw, J. C. (1981). An introduction to the coherence function and its use in EEG signal analysis. *Journal of medical engineering & technology, 5*(6), 279-288.

Sheline, Y. I., Price, J. L., Yan, Z., & Mintun, M. A. (2010). Resting-state functional MRI in depression unmasks increased connectivity between networks via the dorsal nexus. *Proceedings of the National Academy of Sciences, 107*(24), 11020-11025.

Sibille, E., Morris, H. M., Kota, R. S., & Lewis, D. A. (2011). GABA-related transcripts in the dorsolateral prefrontal cortex in mood disorders. *International Journal of Neuropsychopharmacology, 14*(6), 721-734.

Smit, D. J. A., Posthuma, D., Boomsma, D. I., & De Geus, E. J. C. (2007). The relation between frontal EEG asymmetry and the risk for anxiety and depression. *Biological psychology*, *74*(1), 26-33.

Smith, E. E., Cavanagh, J. F., & Allen, J. J. (2018). Intracranial source activity (eLORETA) related to scalp-level asymmetry scores and depression status. *Psychophysiology*, *55*(1), e13019.

Solodkin, A., Zimmermann, J., McIntosh, A. R., Stefanovski, L., & Ritter, P. (2018). Neurological biomarkers and neuroinformatics: the role of the virtual brain. In *Molecular-Genetic and Statistical Techniques for Behavioral and Neural Research* (pp. 3-30). Academic Press.

Song, M., Zhou, Y., Li, J., Liu, Y., Tian, L., Yu, C., & Jiang, T. (2008). Brain spontaneous functional connectivity and intelligence. *Neuroimage*, *41*(3), 1168-1176.

Sporns, O. (2011). The human connectome: a complex network. *Annals of the New York Academy of Sciences*, *1224*(1), 109-125.

Sporns, O. (2014). Contributions and challenges for network models in cognitive neuroscience. *Nature neuroscience*, *17*(5), 652.

Sporns, O., & Betzel, R. F. (2016). Modular brain networks. *Annual review of psychology*, *67*, 613-640.

Srinivasan, R., Winter, W. R., Ding, J., & Nunez, P. L. (2007). EEG and MEG coherence: measures of functional connectivity at distinct spatial scales of neocortical dynamics. *Journal of neuroscience methods*, *166*(1), 41-52.

Stam, C. J., Van Straaten, E. C. W., Van Dellen, E., Tewarie, P., Gong, G., Hillebrand, A., ... & Van Mieghem, P. (2016). The relation between structural and functional connectivity patterns in complex brain networks. *International Journal of Psychophysiology*, *103*, 149-160.

Steyn-Ross, M. L., Steyn-Ross, D. A., Sleigh, J. W., & Liley, D. T. J. (1999). Theoretical electroencephalogram stationary spectrum for a white-noise-driven cortex: evidence for a general anesthetic-induced phase transition. *Physical Review E*, *60*(6), 7299.

Steyn-Ross, M. L., Steyn-Ross, D. A., Sleigh, J. W., & Whiting, D. R. (2003). Theoretical predictions for spatial covariance of the electroencephalographic

signal during the anesthetic-induced phase transition: Increased correlation length and emergence of spatial self-organization. *Physical Review E, 68*(2), 021902.

Strogatz, S. H. (2018). *Nonlinear dynamics and chaos with student solutions manual: With applications to physics, biology, chemistry, and engineering*. CRC press.

Suhhova, A., Bachmann, M., Aadamsoo, K., Võhma, Ü., Lass, J., & Hinrikus, H. (2009). EEG coherence as measure of depressive disorder. *In 4th European Conference of the International Federation for Medical and Biological Engineering* (pp. 353-355). Springer, Berlin, Heidelberg.

Surwillo, W. W. (1961). Frequency of the 'alpha'rhythm, reaction time and age. *Nature, 191*(4790), 823-824.

Surwillo, W. W. (1964). The relation of decision time to brain wave frequency and to age. *Electroencephalography and clinical neurophysiology, 16*(5), 510-514.

Tang, S., Lu, L., Zhang, L., Hu, X., Bu, X., Li, H., ... & Huang, X. (2018). Abnormal amygdala resting-state functional connectivity in adults and adolescents with major depressive disorder: A comparative meta-analysis. *EBioMedicine, 36,* 436-445.

Tement, S., Pahor, A., & Jaušovec, N. (2016). EEG alpha frequency correlates of burnout and depression: The role of gender. *Biological psychology, 114*, 1-12.

Teng, S., Guo, Z., Peng, H., Xing, G., Chen, H., He, B., ... & Mu, Q. (2017). High-frequency repetitive transcranial magnetic stimulation over the left DLPFC for major depression: session-dependent efficacy: a meta-analysis. *European Psychiatry, 41*, 75-84.

Thibodeau, R., Jorgensen, R. S., & Kim, S. (2006). Depression, anxiety, and resting frontal EEG asymmetry: a meta-analytic review. *Journal of abnormal psychology, 115*(4), 715.

Tozzi, L., Zhang, X., Chesnut, M., Holt-Gosselin, B., Ramirez, C. A., & Williams, L. M. (2021). Reduced functional connectivity of default mode network subsystems in depression: Meta-analytic evidence and relationship with trait rumination. *NeuroImage: Clinical, 30,* 102570.

Trevino, K., McClintock, S. M., Fischer, N. M., Vora, A., & Husain, M. M. (2014). Defining treatment-resistant depression: a comprehensive review of the literature. , 26, 3, 26(3), 222-232.

Valiulis, V., Gerulskis, G., Dapsys, K., Vistartaite, G., Siurkute, A., & Maciulis, V. (2012). Electrophysiological differences between high and low frequency rTMS protocols in depression treatment. *Acta Neurobiol Exp, 72*(3), 283-295.

Van Den Heuvel, M. P., Stam, C. J., Kahn, R. S., & Pol, H. E. H. (2009). Efficiency of functional brain networks and intellectual performance. *Journal of Neuroscience*, *29*(23), 7619-7624.

Van Der Vinne, N., Vollebregt, M. A., Van Putten, M. J., & Arns, M. (2017). Frontal alpha asymmetry as a diagnostic marker in depression: Fact or fiction? A meta-analysis. *Neuroimage: clinical*, *16*, 79-87.

Van der Worp, H. B., Kraaier, V., Wieneke, G. H., & Van Huffelen, A. C. (1991). Quantitative EEG during progressive hypocarbia and hypoxia. Hyperventilation-induced EEG changes reconsidered. *Electroencephalography and clinical neurophysiology*, *79*(5), 335-341.

Vieta, E., & Colom, F. (2011). Therapeutic options in treatment-resistant depression. *Annals of medicine*, *43*(7), 512-530.

Virtanen, P., Gommers, R., Oliphant, T. E., Haberland, M., Reddy, T., Cournapeau, D., … SciPy 1.0 Contributors. (2020). SciPy 1.0: Fundamental Algorithms for Scientific Computing in Python. *Nature Methods*, *17*, 261–272. https://doi.org/10.1038/s41592-019-0686-2

von Knorring, L. (1983). Intercorrelations between different computer-based measures of the EEG alpha amplitude and its variability over time and their validity in differentiating healthy volunteers from depressed patients. *Advances in Biological Psychiatry*.

Vriens, E. M., Wieneke, G. H., Van Huffelen, A. C., Visser, G. H., & Eikelboom, B. C. (2000). Increase in alpha rhythm frequency after carotid endarterectomy. *Clinical neurophysiology*, *111*(8), 1505-1513.

Welch, P. (1967). The use of fast Fourier transform for the estimation of power spectra: a method based on time averaging over short, modified periodograms. *IEEE Transactions on audio and electroacoustics*, *15*(2), 70-73.

Willmes, K., Moeller, K., & Klein, E. (2014). Where numbers meet words: a common ventral network for semantic classification. *Scandinavian journal of psychology*, *55*(3), 202-211.

Wu, X. J., Zeng, L. L., Shen, H., Yuan, L., Qin, J., Zhang, P., & Hu, D. (2017). Functional network connectivity alterations in schizophrenia and depression. *Psychiatry Research: Neuroimaging*, *263*, 113-120.

Yadollahpour, A., Hosseini, S. A., & Shakeri, A. (2016). rTMS for the treatment of depression: a comprehensive review of effective protocols on right DLPFC. *International Journal of Mental Health and Addiction*, *14*(4), 539-549.

Youh, J., Hong, J. S., Han, D. H., Chung, U. S., Min, K. J., Lee, Y. S., & Kim, S. M. (2017). Comparison of electroencephalography (EEG) coherence between major depressive disorder (MDD) without comorbidity and MDD comorbid with Internet gaming disorder. *Journal of Korean medical science*, *32*(7), 1160.

Zhang, B., Yan, G., Yang, Z., Su, Y., Wang, J., & Lei, T. (2020). Brain Functional Networks Based on Resting-State EEG Data for Major Depressive Disorder Analysis and Classification. IEEE Transactions on Neural Systems and Rehabilitation Engineering, 29, 215-229.

Zimmermann, J., Perry, A., Breakspear, M., Schirner, M., Sachdev, P., Wen, W., ... & Solodkin, A. (2018). Differentiation of Alzheimer's disease based on local and global parameters in personalized Virtual Brain models. *NeuroImage: Clinical*, *19*, 240-251.

Appendix A

Parameter	Value	Explanation
c_ee	14.05	Excitatory to excitatory coupling coefficient
c_ei	12.44	Inhibitory to excitatory coupling coefficient
c_ie	16.76	Excitatory to inhibitory coupling coefficient.
c_ii	2.0	Inhibitory to inhibitory coupling coefficient.
tau_e	16.07	Excitatory population, membrane time-constant [ms]
tau_i	33.71	Inhibitory population, membrane time-constant [ms]
a_e	1.3	The slope parameter for the excitatory response function
b_e	4.0	Position of the maximum slope of the excitatory sigmoid function
c_e	1.0	The amplitude parameter for the excitatory response function
a_i	1.95	The slope parameter for the inhibitory response function
b_i	14.76	Position of the maximum slope of a sigmoid function [in threshold units]
c_i	1.0	The amplitude parameter for the inhibitory response function
r_e	1.0	Excitatory refractory period
r_i	1.0	Inhibitory refractory period
k_e	1.0	Maximum value of the excitatory response function
k_i	1.0	Maximum value of the inhibitory response function
P	2.22	External stimulus to the excitatory population. Constant intensity.Entry point for coupling.
Q	1.0	External stimulus to the inhibitory population. Constant intensity.Entry point for coupling.
theta_e	0.0	Excitatory threshold
theta_i	0.0	Inhibitory threshold
alpha_e	1.0	External stimulus to the excitatory population. Constant intensity.Entry point for coupling.
alpha_i	1.0	External stimulus to the inhibitory population. Constant intensity.Entry point for coupling.

Appendix A. Overview of the used parameters for the Wilson-Cowan model for all regions in the healthy brain simulations and for all regions except bilateral DLPFC, orbitofrontal and occipital cortices in the other simulations. The excepted regions in the depressed, HF-rTMS and LF-rTMS were modelled with Q = 0, otherwise the parameters had the same values as the healthy model.

Appendix B

Left frontal alpha

Mean and standard deviations

	µHealth	µDepr.	µLF-rTMS	µHF-rTMS	sd Healthy	sd Depr.	sd LF-rTMS	sd HF-rTMS
8-9Hz	4.30E-05	1.39E-04	1.39E-04	6.97E-04	4.99E-05	1.17E-04	1.17E-04	4.87E-04
9-10Hz	1.42E-03	5.90E-03	5.89E-03	8.89E-04	6.46E-04	7.40E-04	7.40E-04	5.28E-04
10-11Hz	2.73E-03	1.08E-03	1.08E-03	2.50E-03	6.15E-04	6.66E-04	6.67E-04	9.66E-04
11-12Hz	6.52E-05	6.12E-05	6.12E-05	1.28E-04	7.60E-05	5.28E-05	5.28E-05	8.01E-05
8-12Hz	8.49E-03	1.43E-02	1.43E-02	7.91E-03	2.45E-04	2.61E-04	2.60E-04	2.14E-03

Effect sizes

	Health_Depr	Health_LF	Health_HF	Depr_LF	Depr_HF	HF_LF
8-9Hz	-1.07	-1.06	-1.88	0.00	1.57	1.57
9-10Hz	-6.42	-6.41	0.89	0.00	-7.75	-7.75
10-11Hz	2.56	2.56	0.28	0.00	1.71	1.70
11-12Hz	0.06	0.06	-0.80	0.00	0.98	0.98
8-12Hz	-22.84	-22.90	0.38	-0.01	-4.17	-4.17

Adjusted p-values

	Health_Depr	Health_LF	Health_HF	Depr_LF	Depr_HF	HF_LF
8-9Hz	3.03E-12	3.87E-12	1.63E-28	1.00E+00	3.38E-22	3.12E-22
9-10Hz	5.89E-106	6.58E-106	6.49E-09	1.00E+00	5.88E-121	6.52E-121
10-11Hz	1.89E-43	2.55E-43	4.91E-02	1.00E+00	5.28E-25	6.40E-25
11-12Hz	6.74E-01	6.71E-01	1.76E-07	1.00E+00	7.04E-11	6.87E-11
8-12Hz	1.85E-211	1.18E-211	1.63E-02	1.00E+00	9.28E-74	9.57E-74

T-statistic

	Health_Depr	Health_LF	Health_HF	Depr_LF	Depr_HF	HF_LF
8-9Hz	-7.55	-7.51	-13.29	-0.03	11.08	11.09
9-10Hz	-45.36	-45.33	6.33	-0.03	-54.83	-54.80
10-11Hz	18.13	18.08	1.98	0.03	12.06	12.04
11-12Hz	0.42	0.43	-5.64	-0.01	6.90	6.90
8-12Hz	-161.52	-161.90	2.67	-0.04	-29.48	-29.48

Appendix C

Right frontal alpha

Mean and standard deviation

	µHealthy	µDepressed	µLF-rTMS	µHF-rTMS	sd Healthy	sd Depressed	sd LF-rTMS	sd HF-rTMS
8-9Hz	4.19E-05	1.44E-04	3.26E-04	1.44E-04	3.08E-05	1.04E-04	2.66E-04	1.03E-04
9-10Hz	1.23E-03	5.95E-03	5.51E-03	5.96E-03	7.00E-04	6.35E-04	5.66E-04	6.30E-04
10-11Hz	2.88E-03	1.09E-03	9.78E-04	1.08E-03	6.21E-04	6.92E-04	5.38E-04	6.88E-04
11-12Hz	6.70E-05	3.57E-05	1.33E-04	3.55E-05	6.70E-05	2.49E-05	7.46E-05	2.49E-05
8-12Hz	8.41E-03	1.44E-03	1.37E-02	1.44E-02	2.76E-04	2.12E-04	2.60E-04	2.13E-04

Effect sizes

	Health_Depr	Health_LF	Health_HF	Depr_LF	Depr_HF	HF_LF
8-9Hz	-1.34	-1.49	-1.34	0.90	0.00	-0.90
9-10Hz	-7.03	-6.69	-7.06	-0.74	0.00	0.75
10-11Hz	2.72	3.26	2.73	-0.17	0.00	0.17
11-12Hz	0.62	-0.93	0.62	1.75	-0.01	-1.75
8-12Hz	-24.21	-19.59	-24.20	-2.97	0.00	2.97

Adjusted p-values

	Health_Depr	Health_LF	Health_HF	Depr_LF	Depr_HF	HF_LF
8-9Hz	2.06E-17	1.14E-20	1.88E-17	4.73E-09	1.00E+00	4.55E-09
9-10Hz	3.06E-113	3.21E-109	1.46E-113	9.32E-07	1.00E+00	7.10E-07
10-11Hz	9.73E-47	1.54E-57	5.14E-47	2.27E-01	1.00E+00	2.36E-01
11-12Hz	2.17E-05	4.33E-10	1.92E-05	1.01E-25	1.00E+00	8.38E-26
8-12Hz	2.06E-216	2.37E-198	2.24E-216	1.23E-51	1.00E+00	1.17E-51

T-statistic

	Health_Depr	Health_LF	Health_HF	Depr_LF	Depr_HF	HF_LF
8-9Hz	-9.44	-10.56	-9.46	6.33	-0.01	-6.34
9-10Hz	-49.74	-47.28	-49.94	-5.21	0.03	5.27
10-11Hz	19.24	23.07	19.34	-1.21	-0.02	1.19
11-12Hz	4.35	-6.57	4.38	12.34	-0.06	-12.37
8-12Hz	-171.17	-138.50	-171.10	-21.02	0.02	21.03

Appendix D

Frontal asymmetry

Mean and standard deviation

	µHealthy	µDepressed	µLF-rTMS	µHF-rTMS	sd Healthy	sd Depressed	sd LF-rTMS	sd HF-rTMS
8-9Hz	2.54	2.35	0.82	8.92	3.77	4.66	1.28	11.39
9-10Hz	1.77	1.00	1.09	0.15	1.79	0.18	0.20	0.10
10-11Hz	1.04	2.33	1.62	5.00	0.51	3.86	1.60	7.15
11-12Hz	3.56	3.55	0.75	7.06	6.65	6.16	1.03	7.75
8-12Hz	1.01	0.99	1.04	0.55	0.04	0.03	0.03	0.15

Effect sizes

	Health_Depr	Health_LF	Health_HF	Depr_LF	Depr_HF	HF_LF
8-9Hz	0.05	0.61	-0.75	-0.45	0.75	0.99
9-10Hz	0.60	0.53	1.27	0.43	-5.96	-5.90
10-11Hz	-0.47	-0.49	-0.78	-0.24	0.46	0.65
11-12Hz	0.00	0.59	-0.48	-0.63	0.50	1.13
8-12Hz	0.52	-0.95	4.15	1.78	-4.06	-4.51

Adjusted p-values

	Health_Depr	Health_LF	Health_HF	Depr_LF	Depr_HF	HF_LF
8-9Hz	1.00E+00	1.05E-04	6.43E-07	5.61E-03	8.56E-07	6.37E-11
9-10Hz	1.82E-04	4.33E-04	9.33E-16	5.61E-03	3.71E-100	2.38E-99
10-11Hz	3.44E-03	6.93E-04	3.32E-07	9.35E-02	1.23E-03	7.59E-06
11-12Hz	1.00E+00	1.46E-04	7.97E-04	5.42E-05	1.07E-03	2.69E-13
8-12Hz	1.17E-03	9.22E-10	2.64E-73	2.06E-26	5.62E-72	2.57E-79

T-statistic

	Health_Depr	Health_LF	Health_HF	Depr_LF	Depr_HF	HF_LF
8-9Hz	0.32	4.31	-5.29	-3.15	5.32	7.03
9-10Hz	4.22	3.77	8.97	3.05	-42.16	-41.72
10-11Hz	-3.30	-3.45	-5.51	-1.69	3.28	4.60
11-12Hz	0.01	4.15	-3.41	-4.46	3.52	8.02
8-12Hz	3.69	-6.72	29.33	12.60	-28.74	-31.88

Dutch summary

Een depressie is een ernstig mentaal probleem waar veel mensen aan lijden. Eerder onderzoek vond evidentie voor veranderingen in functionele en structurele connectiviteit en veranderingen in neurotransmitters in de hersenen van patiënten met depressie. De literatuur hieromtrent is echter niet eenduidig, mogelijks door het gebruik van kleine groepen, interindividuele verschillen en conductie-problemen bij het verzamelen van data. In de huidige studie maken we gebruik van modellen om de veranderingen in het depressieve brein en de effecten van niet-invasieve hersenstimulatie te onderzoeken doormiddel van The Virtual Brain (TVB). TVB is een neuro-informatica platform waarmee een persoonlijk virtueel brein kan worden gemodelleerd voor ieder individueel subject, gebaseerd op individueel tractografische data en neurale modellen. Omwille van het gebrek aan echte patiënten, maakten wij gebruik van de standaard connectiviteitsmatrix die in TVB beschikbaar is en modelleerden we hersenactiviteit met behulp van het Wilson-Cowan model. We simuleerden hersenactiviteit voor 4 groepen: 1) Gezond brein, 2) Depressief brein, 3) Depressief brein met high-frequency rTMS en 4) Depressief brein met low-frequency rTMS. Voor iedere groep werden 100 unieke simulaties gemaakt. Vervolgens vergeleken we de groepen in termen van alfa power, coherentie en individuele alfa piek om te onderzoeken 1) of gezonde en depressieve hersenen verschilden zoals verwacht op basis van literatuur, 2) of rTMS protocollen een behandelings-effect konden opleveren en 3) zo ja, of één type rTMS superieure resultaten opleverde vergeleken met het andere type. Onze resultaten waren ambigu en niet geheel in lijn met onze verwachtingen op basis van literatuur. We konden bijvoorbeeld niet altijd de voorspelde verschillen tussen gezonde en depressieve breinen terugvinden en behandelings-effecten waren zeldzaam. We argumenteren dat ons model voor het depressieve brein mogelijks te simplistisch was en moedigen het gebruik van data van echte patiënten in TVB aan voor toekomstig onderzoek. Als laatste benadrukken we enkele problemen en inconsistenties tussen studies die mogelijks de diverse conclusies in de literatuur kunnen verklaren.